CERN-EP-2021-114
2021/07/28

CMS-SUS-20-003

Search for chargino-neutralino production in events with Higgs and W bosons using 137 fb^{-1} of proton-proton collisions at $\sqrt{s} = 13 \text{ TeV}$

The CMS Collaboration*

Abstract

A search for electroweak production of supersymmetric (SUSY) particles in final states with one lepton, a Higgs boson decaying to a pair of bottom quarks, and large missing transverse momentum is presented. The search uses data from proton-proton collisions at a center-of-mass energy of 13 TeV collected using the CMS detector at the LHC, corresponding to an integrated luminosity of 137 fb^{-1} . The observed yields are consistent with backgrounds expected from the standard model. The results are interpreted in the context of a simplified SUSY model of chargino-neutralino production, with the chargino decaying to a W boson and the lightest SUSY particle (LSP) and the neutralino decaying to a Higgs boson and the LSP. Charginos and neutralinos with masses up to 820 GeV are excluded at 95% confidence level when the LSP mass is small, and LSPs with mass up to 350 GeV are excluded when the masses of the chargino and neutralino are approximately 700 GeV.

Submitted to the Journal of High Energy Physics

1 Introduction

Supersymmetry (SUSY) [1–3] is an appealing extension of the standard model (SM) that predicts the existence of a superpartner for every SM particle, with the same gauge quantum numbers but differing by one half unit of spin. SUSY allows addressing several shortcomings of the SM. For example, the superpartners can play an important role in stabilizing the mass of the Higgs boson (H) [4, 5]. In R -parity conserving SUSY models, the lightest supersymmetric particle (LSP) is stable and therefore is a viable dark matter candidate [6].

The SUSY partners of the SM gauge bosons and the Higgs boson are known as winos (partners of the $SU(2)_L$ gauge fields), the bino (partner of the $U(1)$ gauge field), and higgsinos. Neutralinos ($\tilde{\chi}^0$) and charginos ($\tilde{\chi}^\pm$) are the corresponding mass eigenstates of the winos, bino and higgsinos. They do not carry color charge and are therefore produced only via electroweak interactions or in the decay of colored superpartners. Because of the smaller cross sections for electroweak processes, the masses of these particles are experimentally less constrained than the masses of colored SUSY particles. Depending on the mass spectrum, the neutralinos and charginos can have significant decay branching fractions to vector or scalar bosons. In particular, the decays via the W and the Higgs boson are expected to be significant if the $\tilde{\chi}_1^0$ and $\tilde{\chi}_2^0$ particles are wino-like, the $\tilde{\chi}_1^\pm$ is bino-like, and the difference between their masses is larger than the Higgs boson mass, where the subscript 1 2 denotes the lightest (second lightest) neutralino or chargino, respectively. These considerations strongly motivate a search for the electroweak production of SUSY partners presented in this paper.

This paper reports the results of a search for chargino-neutralino production with subsequent $\tilde{\chi}_1^\pm \rightarrow W^\pm \tilde{\chi}_1^0$ and $\tilde{\chi}_2^0 \rightarrow H \tilde{\chi}_1^0$ decays, as shown in Fig. 1. The data analysis focuses on the final state with a charged lepton produced in the W boson decay, two jets reconstructed from the $H \rightarrow b\bar{b}$ decay, and significant missing transverse momentum (p_T^{miss}) resulting from the LSPs and the neutrino. This final state benefits from the large branching fraction for $H \rightarrow b\bar{b}$, 58%. The chargino and neutralino are assumed to be wino-like, and the $\tilde{\chi}_1^0$ produced in their decays is assumed to be the stable LSP. As wino-like charginos $\tilde{\chi}_1^\pm$ and neutralinos $\tilde{\chi}_2^0$ would be nearly degenerate, this analysis considers a simplified model [7–9] with a single mass parameter for both the chargino and neutralino ($m_{\tilde{\chi}_{2/1}^0}$), as well as an additional mass parameter for the LSP ($m_{\tilde{\chi}_1^0}$). Results of searches in this final state were previously presented by ATLAS [10, 11] and CMS [12–14] using data sets at center of mass energy 8 and 13 TeV.

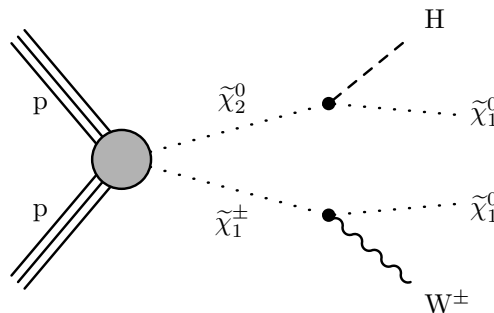


Figure 1: Diagram for a simplified SUSY model with electroweak production of the lightest chargino $\tilde{\chi}_1^\pm$ and next-to-lightest neutralino $\tilde{\chi}_2^0$. The $\tilde{\chi}_1^\pm$ decays to a W boson and the lightest neutralino $\tilde{\chi}_1^0$. The $\tilde{\chi}_2^0$ decays to a Higgs boson and a $\tilde{\chi}_1^0$.

This analysis uses 13 TeV proton-proton (pp) collision data collected with the CMS detector during the 2016–2018 data-taking periods, corresponding to an integrated luminosity of 137 fb^{-1} .

Relative to the most recent result from the CMS Collaboration targeting this signature [12], the results significantly extend the sensitivity to the mass of the chargino and neutralino. The improved sensitivity is achieved through a nearly four-fold increase in the integrated luminosity, as well as from numerous improvements in the analysis, including the addition of a discriminant that identifies Higgs boson decays collimated into large-radius jets, regions that include additional jets from the initial-state radiation, and an expanded categorization in p_T^{miss} .

2 The CMS detector

The central feature of the CMS apparatus is a superconducting solenoid of 6 m internal diameter, providing a magnetic field of 3.8 T. Within the solenoid volume are a silicon pixel and strip tracker, a lead tungstate crystal electromagnetic calorimeter, and a brass and scintillator hadron calorimeter, each composed of a barrel and two endcap sections. Forward calorimeters extend the pseudorapidity (η) coverage provided by the barrel and endcap detectors. Muons are detected in gas-ionization chambers embedded in the steel flux-return yoke outside the solenoid. A more detailed description of the CMS detector, together with a definition of the coordinate system used and the relevant kinematic variables, can be found in Ref. [15].

Events of interest are selected using a two-tiered trigger system. The first level, composed of custom hardware processors, uses information from the calorimeters and muon detectors to select events at a rate of approximately 100 kHz within a fixed time interval of about 4 ns [16]. The second level, known as the high-level trigger, consists of a farm of processors running a version of the full event reconstruction software optimized for fast processing, and reduces the event rate to approximately 1 kHz before data storage [17].

3 Simulated samples

Monte Carlo (MC) simulation is used to design the search strategy, study and estimate SM backgrounds, and evaluate the sensitivity of the analysis to the SUSY signal. Separate MC simulations are used to reflect the detector configuration and running conditions of different periods (2016, 2017, and 2018). The MADGRAPH5_aMC@NLO 2 (versions 2.2.2 for 2016 and 2.4.2 for 2017–2018) generator [18] at leading order (LO) in quantum chromodynamics (QCD) is used to generate samples of events of SM $t\bar{t}$, W +jets, and WH processes, as well as chargino-neutralino production, as described by a simplified model of SUSY. Samples of W +jets, $t\bar{t}$, and SUSY events are generated with up to four, three, and two additional partons included in the matrix-element calculations, respectively. The MADGRAPH5_aMC@NLO generator at next-to-leading-order (NLO) in QCD is used to generate samples of $t\bar{t}Z$ and WZ events, while single top quark events are generated at NLO in QCD using the POWHEG 2.0 [19–22] program.

The NNPDF3.0 (3.1) parton distribution functions, PDFs, are used to generate all 2016 (2017–2018) MC samples [23–25]. The parton shower and hadronization are modeled with PYTHIA 8.226 (8.230) [26] in 2016 (2017–2018) samples. The MLM [27] and FxFx [28] prescriptions are employed to match partons from the matrix-element calculation to those from the parton showers for the LO and NLO samples, respectively.

The 2016 MC samples are generated with the CUETP8M1 PYTHIA tune [29]. For later data-taking periods, the CP5 and CP2 tunes [30] are used for SM and SUSY signal samples, respectively. The GEANT4 [31] package is used to simulate the response of the CMS detector for all SM processes, while the CMS fast simulation program [32, 33] is used for signal samples.

Cross section calculations performed at next-to-next-to-leading-order (NNLO) in QCD are used

to normalize the MC samples of W+jets [34], and at NLO in QCD to normalize single top quark samples [35, 36]. The $t\bar{t}$ samples are normalized to a cross section determined at NNLO in QCD that includes the resummation of the next-to-next-to-leading-logarithmic soft-gluon terms [37–43]. MC samples of other SM background processes are normalized to cross sections obtained from the MC event generators at either LO or NLO in QCD. Cross sections for wino-like chargino-neutralino production are computed at approximate NLO plus next-to-leading logarithmic (NLL) precision. Other SUSY particles except for the LSP are assumed to be heavy and decoupled [44–47]. A SM-like $H \rightarrow b\bar{b}$ branching fraction of 58.24% [48] is assumed.

Nominal distributions of additional pp collisions in the same or adjacent bunch crossings (pileup) are used in the generation of simulated samples. These samples are reweighted such that the number of interactions per bunch crossing matches the observation.

4 Event selection and search strategy

In order to search for the chargino-neutralino production mechanism shown in Fig. 1, the analysis targets decay modes of the W boson to leptons and the H to a bottom quark-antiquark pair. The analysis considers events with a single isolated electron or muon, two jets identified as originating from two bottom quarks, and large p_T^{miss} from the LSPs and the neutrino. The major backgrounds in this final state arise from SM processes containing top quarks and W bosons. These backgrounds are suppressed with the analysis strategy described below that uses physics objects summarized in Table 1, which are similar to those presented in Ref. [49].

Events are reconstructed using the particle-flow (PF) algorithm [50], which combines information from the CMS subdetectors to identify charged and neutral hadrons, photons, electrons, and muons, collectively referred to as PF candidates. These candidates are associated with reconstructed vertices, and the vertex with the largest sum of squared physics-object transverse momenta is taken to be the primary pp interaction vertex. The physics objects used for the primary vertex determination include a special collection of jets reconstructed by clustering only tracks associated to the vertex, and the magnitude of the associated missing transverse momentum. The missing transverse momentum in this case is defined as the negative vector sum of the transverse momentum (p_T) of the jets in this collection. In all other cases, the missing transverse momentum (p_T^{miss}) is taken as the negative vector sum of the p_T of all PF candidates, excluding charged hadron candidates that do not originate from the primary vertex [51].

Electron candidates are reconstructed by combining clusters of energy deposits in the electromagnetic calorimeter with charged tracks [52]. The electron identification is performed using shower shape variables, track-cluster matching variables, and track quality variables. The selection on these variables is optimized to identify electrons from the decay of W and Z bosons while rejecting electron candidates originating from jets. To reject electrons originating from photon conversions inside the detector, electrons are required to have at most one missing measurement in the innermost tracker layers and to be incompatible with any conversion-like secondary vertices. Muon candidates are reconstructed by geometrically matching tracks from measurements in the muon system and tracker, and fitting them to form a global muon track. Muons are selected using the quality of the geometrical matching and the quality of the tracks [53].

Selected muons (electrons) are required to have $p_T \geq 25$ (30) GeV, $\eta \in [2.1, 1.44]$, and be isolated. Events containing electrons with $\eta < 1.44$ have been found to exhibit an anomalous tail in the transverse mass distribution and are not included in the search. Lepton isolation is determined from the scalar p_T sum (p_T^{sum}) of PF candidates not associated with the lepton

within a cone of p_T -dependent radius starting at $\Delta R = \sqrt{\Delta^2 + \Delta^2} = 0.2$, where Δ is the azimuthal angle in radians. This radius is reduced to $\Delta R = \max(0.05, 10 \text{ GeV}/p_T)$ for a lepton with $p_T = 50 \text{ GeV}$. Leptons are considered isolated if the scalar p_T sum within this radius is less than 10% of the lepton p_T . Additionally, leptons are required to have a scalar p_T sum within a fixed radius of $\Delta R = 0.3$ less than 5 GeV. Typical lepton selection efficiencies are approximately 85% for electrons and 95% for muons, depending on the p_T and Δ of the lepton.

Events containing a second lepton passing a looser “veto lepton” selection, a τ passing a “veto tau” selection, or an isolated charged PF candidate are rejected. Hadronic τ decays are identified by a multi-variate analysis (MVA) isolation algorithm that selects both one- and three-pronged topologies and allows for the presence of additional neutral pions [54, 55]. These vetoes are designed to provide additional rejection against events containing two leptons, or a lepton and a hadronic τ decay.

Hadronic jets are reconstructed from neutral and charged PF candidates associated with the primary vertex, using the anti- k_T clustering algorithm [56, 57]. Two collections of jets are produced, with different values of the distance parameter R . Both collections of jets are corrected for contributions from event pileup and the effects of nonuniform detector response [58].

“Small- R ” jets are reconstructed with a distance parameter $R = 0.4$, and aim to reconstruct jets arising from a single parton. Selected small- R jets have $p_T = 30 \text{ GeV}$, $\Delta = 2.4$, and are separated from isolated leptons by $\Delta R = 0.4$. Small- R jets that contain the decay of a b-flavored hadron are identified as bottom quark jets (b-tagged jets) using a deep neural network algorithm, DEEPCSV. The discriminator working point is chosen so that the misidentification rate to tag light-flavor or gluon jets is approximately 1–2%. This choice results in an efficiency to identify a bottom quark jet in the range 65–80% for jets with p_T between 30 and 400 GeV, and an efficiency of 10–15% for jets originating from a charm quark. The b tagging efficiency in simulation is corrected using scale factors derived from comparisons of data with simulation in control samples [59].

When the p_T of the Higgs boson is not too large compared to its mass, the b jets resulting from its decay to bottom quarks are spatially separated. As the Higgs boson p_T increases, the separation between the b jets decreases. For the SUSY signal, this becomes important when the mass splitting between the neutralino $\tilde{\chi}_2^0$ and the LSP is large. To improve the sensitivity to large $\tilde{\chi}_2^0$ masses, a second collection of “large- R ” jets is formed with distance parameter $R = 0.8$.

Selected large- R jets have $p_T = 250 \text{ GeV}$, $\Delta = 2.4$, and are separated from isolated leptons by $\Delta R = 0.8$. Large- R jets containing a candidate $H \rightarrow b\bar{b}$ decay are identified as H-tagged jets using a dedicated deep neural network algorithm [60]. We use the mass-decorrelated version of the DEEPAK8 algorithm, which considers the properties of jet constituent particles and secondary vertices. The imposed requirement on the neural network score corresponds to a misidentification rate of approximately 2.5% for large- R jets with a p_T of 500–700 GeV without an $H \rightarrow b\bar{b}$ decay in multijet events. The efficiency to identify an H decay to bottom quarks is 60–80% depending on the p_T of the large- R jet.

The p_T^{miss} is modified to account for corrections to the energy scale of the reconstructed jets in the event. Events with possible p_T^{miss} contributions from beam halo interactions or anomalous noise in the calorimeter are rejected using dedicated filters [61]. Additionally, during part of the 2018 data-taking period, two sectors of the endcap hadronic calorimeter experienced a power loss, affecting approximately 39 fb^{-1} of data. As the identification of both electrons and jets depends on correct energy fraction measurements, events from the affected data-taking periods

containing an electron or a jet in the region $2.4 < \Delta R < 1.4$ and $1.6 < \Delta R < 0.8$ are rejected. The total loss in signal efficiency considering all event filters is less than 1%.

Data events are selected using a logical “or” of triggers that require either the presence of an isolated electron or muon; or large p_T^{miss} and H_T^{miss} , where H_T^{miss} is the magnitude of the negative vector p_T sum of all jets and leptons. The combined trigger efficiency, measured with an independent data sample of events with a large scalar p_T sum of small- R jets, is greater than 99% for events with $p_T^{\text{miss}} > 225$ GeV and lepton $p_T > 20$ GeV. The trigger requirements are summarized in Table 2.

Table 3 defines the event preselection common to all signal regions, which requires exactly one isolated lepton, $p_T^{\text{miss}} > 125$ GeV, two or three small- R jets, and no isolated tracks or veto tau candidates.

Exactly two of the small- R jets must be b-tagged. The primary SM processes that contribute to the preselection region are $t\bar{t}$, single top quark (mostly in the tW channel), and W +jets production.

The SM processes with one W boson that decays to leptons, originating primarily from semileptonic $t\bar{t}$ and W +jets, are suppressed by requiring the transverse mass, m_T , to be greater than 150 GeV. m_T is defined as

$$m_T = \sqrt{2p_T p_T^{\text{miss}} (1 - \cos \Delta)}, \quad (1)$$

where p_T denotes the lepton p_T and Δ is the azimuthal separation between p_T and p_T^{miss} . After requiring a large m_T , the dominant remaining background comes from processes with two W bosons that decay to leptons (including τ leptons), primarily $t\bar{t}$ and tW . To suppress

Table 1: Summary of the requirements for the physics objects used in this analysis.

| | |
|------------------------------|--|
| Lepton | e with $p_T > 25$ GeV, $2.1 < \Delta R < 1.44$ $p_T^{\text{sum}} > 0.1 p_T, p_T^{\text{sum}} > 5$ GeV |
| Veto lepton | or e with $p_T > 5$ GeV, $2.4 < \Delta R < 2.4$ $p_T^{\text{sum}} > 0.2 p_T$ |
| Veto track | charged PF candidate, $p_T > 10$ GeV, $2.4 < \Delta R < 2.4$ $p_T^{\text{sum}} > 0.1 p_T, p_T^{\text{sum}} > 6$ GeV |
| Veto h | hadronic h with $p_T > 10$ GeV, $2.4 < \Delta R < 2.4$ h MVA isolation |
| Jets | anti- k_T jets, $R = 0.4$, $p_T > 30$ GeV, $2.4 < \Delta R < 2.4$ anti- k_T jets, $R = 0.8$, $p_T > 250$ GeV, $2.4 < \Delta R < 2.4$ |
| b tagging | DEEPCSV algorithm (1% misidentification rate) |
| H tagging | mass-decorrelated H tagging discriminator |
| p_T^{sum} cone size | relative isolation: $\Delta R > \min \max (0.05, 10 \text{ GeV}/p_T)$, $0.2 < \Delta R < 0.2$ veto track, and absolute isolation: $\Delta R > 0.3$ |

Table 2: Summary of the triggers used to select the analysis data set. Events are selected using a logical “or” of the following triggers.

| | | |
|---------------------|---------------------------------|-----------------------|
| p_T^{miss} | 120 GeV and H_T^{miss} | 120 GeV (2016–2018) |
| p_T^{miss} | 170 GeV | (2016) |
| Isolated e | with p_T | 24 25 GeV (2016) |
| Isolated e | with p_T | 24 35 GeV (2017–2018) |

these backgrounds, events with an additional veto lepton or a hadronic decay are rejected, as described above.

Additional background rejection is obtained using the cotransverse mass variable, m_{CT} , which is defined as

$$m_{\text{CT}} = \sqrt{2p_T^{b_1} p_T^{b_2} (1 - \cos \Delta_{b\bar{b}})}, \quad (2)$$

where $p_T^{b_1}$ and $p_T^{b_2}$ are the magnitudes of the transverse momenta of the two b-tagged jets and $\Delta_{b\bar{b}}$ is the azimuthal angle between the two b-tagged jets [62]. This variable has a kinematic endpoint close to 150 GeV for $t\bar{t}$ events when both b jets are correctly identified, while signal events tend to have higher values of m_{CT} . Requiring $m_{\text{CT}} > 200$ GeV is effective at reducing the dilepton $t\bar{t}$ and tW backgrounds.

Table 3: Summary of the preselection requirements common to all signal regions. The N_b is the multiplicity of b-tagged jets and $p_T^{\text{non-b}}$ is the p_T of the non-b-tagged jet.

| | |
|---------------------|--|
| Lepton | Single e or μ and no additional veto lepton, track or tau |
| Small-R jets | $2 < N_{\text{jets}} < 3$, $N_b = 2$, $p_T^{\text{non-b}} > 300$ GeV |
| p_T^{miss} | 125 GeV |
| $m_{b\bar{b}}$ | 90–150 GeV |
| m_T | 150 GeV |
| m_{CT} | 200 GeV |

Events entering the signal regions must pass the preselection and satisfy the m_T and m_{CT} requirements above. We also require that the invariant mass of the pair of b-tagged jets, $m_{b\bar{b}}$, be between 90 and 150 GeV, consistent with the mass of an SM Higgs boson. In events with 3 small-R jets, the non-b-tagged jet must have $p_T > 300$ GeV. This requirement rejects some $t\bar{t}$ events that survive the m_{CT} and p_T^{miss} selections. These requirements define the baseline signal selection. Figure 2 shows the distributions of p_T^{miss} , m_{CT} , $m_{b\bar{b}}$, m_T , the number of small-R jets (N_{jets}), and the discriminator output of the H tagging algorithm in simulated signal and background samples. All preselection requirements specified in Table 3 are applied except the one on the plotted variable, illustrating the discrimination power of each variable.

Events passing the baseline signal selection are further categorized into signal regions according to N_{jets} , the number of H-tagged large-R jets N_H , and the value of p_T^{miss} . The twelve non-overlapping signal regions are defined in Table 4.

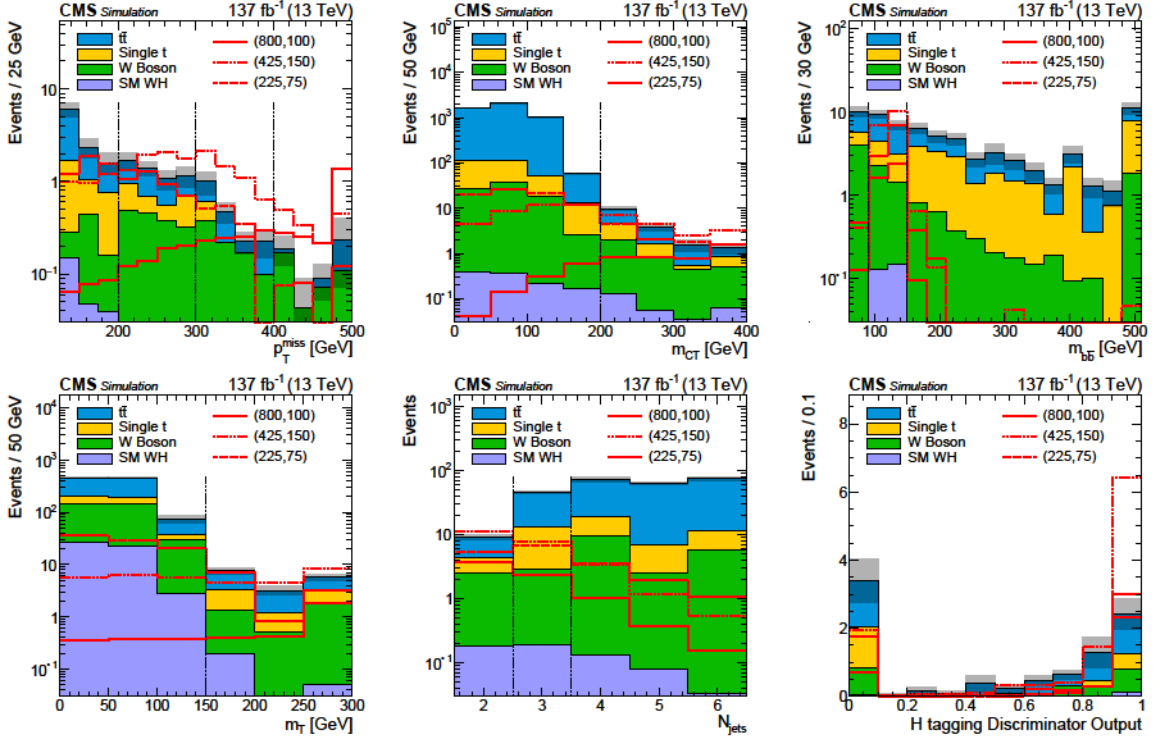


Figure 2: Distributions of p_T^{miss} , m_{CT} , $m_{b\bar{b}}$, m_T , N_{jets} , and the $H \rightarrow b\bar{b}$ large- R jet discriminator in simulated background and signal samples. Three benchmark signal points corresponding to masses in GeV ($m_{\tilde{\chi}_2^0/\tilde{\chi}_1^\pm}$, $m_{\tilde{\chi}_1^0}$) of (800, 100), (425, 150) and (225, 75) are shown as solid, dashed, and short-dashed lines, respectively. Events are taken from the 2-jet signal regions with $p_T^{\text{miss}} > 125$ GeV, with all of the requirements specified in Table 3 except for the one on the plotted variable. The shaded areas correspond to the statistical uncertainty of the simulated backgrounds. The dashed vertical lines indicate the thresholds used to define the signal regions. These indicators are not shown on the H tagging discriminator score distribution because the required values vary between 0.83 and 0.90, depending on the data-taking year.

Table 4: Definition of the 12 non-overlapping signal regions categorized in N_H , N_{jets} , and p_T^{miss} , where N_H is the number of large- R jets tagged as $H \rightarrow b\bar{b}$.

| N_H | N_{jets} | p_T^{miss} [GeV] |
|-------|-------------------|--|
| 0 | 2, 3 | [125, 200), [200, 300), [300, 400), [400, ∞) |
| 1 | 2, 3 | [125, 300), [300, ∞) |

5 Background estimation

There are two dominant background categories relevant for this search: top quark production and W boson production. The contributions of these backgrounds to the yields in the signal regions are estimated using observed yields in control regions (CRs) and transfer factors obtained from simulated samples. The transfer factors are validated in non-overlapping regions adjacent to the signal regions. The top quark backgrounds include $t\bar{t}$ pair production, single top quark production (tW), and a small contribution from $t\bar{t}W$ and $t\bar{t}Z$ production. These backgrounds dominate in the lower- p_T^{miss} search regions and are estimated from CRs in data using the method described in Section 5.1. In the high- p_T^{miss} regions, W boson production becomes

the dominant background. The method described in Section 5.2 estimates the background arising from W +jets, WW , and WZ production using CRs in data. The remaining background arises from standard model WH production. This process contributes less than 5% of the total background in any of the search regions, and its yield is estimated from simulation. A 25% uncertainty in the cross section of this process is assigned, based on the uncertainty in the WH cross section measurement [63].

5.1 Top quark background

Events containing top quarks constitute the dominant background, particularly in bins with $N_{\text{jets}} = 3$ or low $p_{\text{T}}^{\text{miss}}$. These events contain b jets and isolated leptons from W bosons, so they lead to similar final states as the signal. Owing to the high m_{T} requirement, the majority of the top quark background stems from events with two leptonically decaying W bosons. In this case, one of the leptons either is not reconstructed, fails the identification requirements, is not isolated, or is outside of kinematic acceptance.

The $t\bar{t}$ background is further suppressed by the m_{CT} requirement, which has an endpoint at approximately 150 GeV for $t\bar{t}$ events in the case when both daughter b jets are reconstructed and identified. The m_{CT} value for $t\bar{t}$ events can exceed the cutoff for three reasons: (i) if there are mistagged light-flavor jets or extra b jets, (ii) if a b jet is reconstructed with excess p_{T} because it overlaps with other objects, or (iii) because of excess b jet p_{T} arising due to the finite jet energy resolution.

A control sample enriched in top quark events is obtained by inverting the m_{CT} requirement. For each signal region (SR), we form a corresponding control region spanning a range of m_{CT} from 100 to 200 GeV. These CRs are used to normalize the top quark background to data in a single-lepton, high- m_{T} region in each bin of $p_{\text{T}}^{\text{miss}}$, N_{H} , and N_{jets} . In each CR, a transfer factor from MC simulation (R_{top}) is used to extrapolate the yield for the corresponding high- m_{CT} signal regions. The top quark background estimate is then given by

$$N_{\text{SR}}^{\text{top}}(p_{\text{T}}^{\text{miss}}, N_{\text{jets}}, N_{\text{H}}) = R_{\text{top}}(p_{\text{T}}^{\text{miss}}, N_{\text{jets}}, N_{\text{H}}) N_{\text{CR}}^{\text{obs.}}(p_{\text{T}}^{\text{miss}}, N_{\text{jets}}, N_{\text{H}}), \quad (3)$$

where the $N_{\text{SR}}^{\text{top}}$ is the number of expected events in the SR, $N_{\text{CR}}^{\text{obs.}}$ is the number of observed events in the CR, and R_{top} are defined as

$$R_{\text{top}}(p_{\text{T}}^{\text{miss}}, N_{\text{jets}}, N_{\text{H}}) = \frac{N_{\text{SR}}^{\text{top MC}}(p_{\text{T}}^{\text{miss}}, N_{\text{jets}}, N_{\text{H}})}{N_{\text{CR}}^{\text{SM MC}}(p_{\text{T}}^{\text{miss}}, N_{\text{jets}}, N_{\text{H}})}. \quad (4)$$

The $N_{\text{SR}}^{\text{top MC}}$ and $N_{\text{CR}}^{\text{SM MC}}$ are the expected top quark and total SM yields in the signal and control regions, respectively, according to simulation.

The contamination from other processes (primarily W boson production) in the low- m_{CT} CRs is as low as 2% in the lower- $p_{\text{T}}^{\text{miss}}$ regions, growing to 25% in the highest $p_{\text{T}}^{\text{miss}}$ control region. This contamination is included in the denominator of R_{top} as shown in Eq. (4). Additionally, to increase the expected yields in the CRs, two modifications to the CR definitions are made. First, for the CRs with an H-tagged large- R jet, the m_{CT} lower bound is removed (for a total range of 0–200 GeV). Second, for CRs with $p_{\text{T}}^{\text{miss}} > 300$ GeV, the $m_{b\bar{b}}$ window is expanded to 90–300 GeV.

The data yields, transfer factors, and the resulting top quark background predictions are summarized in Table 5. These predictions, combined with the other background estimates, are compared with the observed yields in Section 6.

Table 5: The values of the R_{top} transfer factors, the observed yields in the low- m_{CT} CRs, and the resulting top quark background prediction in each bin of $p_{\text{T}}^{\text{miss}}$, N_{jets} , and N_{H} . The uncertainty shown for R_{top} is only of statistical origin. For the top quark prediction both the statistical and systematic uncertainties are shown (discussed in the text.)

| N_{jets} | N_{H} | $p_{\text{T}}^{\text{miss}}$ [GeV] | R_{top} | | $N_{\text{CR}}^{\text{obs.}}$ | $N_{\text{SR}}^{\text{top}}$ | | | |
|-------------------|----------------|------------------------------------|------------------|-------|-------------------------------|------------------------------|------|------|-----|
| 2 | 0 | 125–200 | 0.006 | 0.001 | 978 | 6.3 | 0.9 | 0.9 | |
| | | 200–300 | 0.015 | 0.003 | 161 | 2.4 | 0.5 | 0.4 | |
| | | 300–400 | 0.05 | 0.02 | 6 | 0.3 | 0.1 | 0.1 | |
| | | 400 | 0.02 | 0.02 | 1 | 0.02 | 0.02 | 0.01 | |
| | 1 | 125–300 | 0.26 | 0.06 | 6 | 1.6 | 0.8 | 0.4 | |
| | | 300 | 0.03 | 0.01 | 11 | 0.4 | 0.2 | 0.3 | |
| | 3 | 0 | 125–200 | 0.020 | 0.002 | 851 | 17.5 | 1.6 | 2.6 |
| | | | 200–300 | 0.05 | 0.01 | 151 | 7.1 | 1.1 | 1.3 |
| 300–400 | | | 0.04 | 0.01 | 19 | 0.8 | 0.3 | 0.3 | |
| 400 | | | 0.2 | 0.2 | 1 | 0.2 | 0.2 | 0.1 | |
| 1 | | 125–300 | 0.28 | 0.05 | 18 | 5.0 | 1.4 | 1.4 | |
| | | 300 | 0.12 | 0.03 | 14 | 1.7 | 0.7 | 1.4 | |

To assess the modeling of the top quark background, we conduct a validation test in a sideband requiring $m_{\text{b}\bar{\text{b}}} > 150$ GeV and the same m_{CT} and m_{T} requirements as the SR. The relative contributions from SM processes are similar in the sideband and the signal regions. The modeling of the top quark background in this region is also affected by the same sources of uncertainty, including the imperfect knowledge of the object efficiencies, jet energy scale and resolution, and the distribution of additional pileup interactions. An analogous background prediction is performed in this region, and the level of agreement observed is used to derive a systematic uncertainty in the R_{top} factors.

The yields in the $m_{\text{b}\bar{\text{b}}} > 150$ GeV validation regions (VRs) are estimated using CRs defined with the same m_{T} and m_{CT} requirements as the CRs for the SR predictions: $m_{\text{T}} > 150$ GeV, and $m_{\text{CT}} > 100$ GeV for $N_{\text{H}} = 0, 1$. Two modifications are introduced to improve the statistical precision of the test: first, the $N_{\text{jets}} = 2$ and $N_{\text{jets}} = 3$ bins are combined; and second, all regions with $p_{\text{T}}^{\text{miss}} > 300$ GeV and $p_{\text{T}}^{\text{miss}} > 400$ GeV are combined. Additionally, to avoid overlap with the low- m_{CT} control regions used to estimate the top quark background in the SR, the low- m_{CT} regions used for the VR predictions in bins with $p_{\text{T}}^{\text{miss}} > 300$ GeV are restricted to $m_{\text{b}\bar{\text{b}}} > 300$ GeV.

A comparison of the R_{top} factors obtained from data and simulation in the VRs is shown in Fig. 3. Good agreement is observed, and we assign the statistical uncertainties in the differences of the observed and simulated values as the systematic uncertainties in the corresponding R_{top} factors. These uncertainties reflect the degree to which we can evaluate the modeling of R_{top} factors in data. This validation approach has the advantage of probing both the known sources of uncertainty as well as any unknown sources that could affect the m_{CT} extrapolation. The uncertainties derived from this test, together with those associated with the finite yields in the low- m_{CT} CRs and the MC statistical precision form the complete set of uncertainties assigned to the top quark background prediction.

Additional cross-checks of the top quark background estimate are performed in a dilepton validation region and in a region with exactly one b jet. These studies are performed in all 12 bins

of p_T^{miss} , N_{jets} , and N_H , and the results agree with those obtained from the studies performed in the $m_{b\bar{b}}$ sideband. A second, independent estimate of the top quark background is performed following the “lost-lepton” method described in Ref. [49]. In this method, the contribution from top quark processes in each signal region is normalized using a corresponding control region requiring two leptons and all other signal region selections. The estimates obtained from the two methods are consistent. These additional cross-checks are not used quantitatively to determine uncertainties, but they build confidence in the modeling of the R_{top} factors.

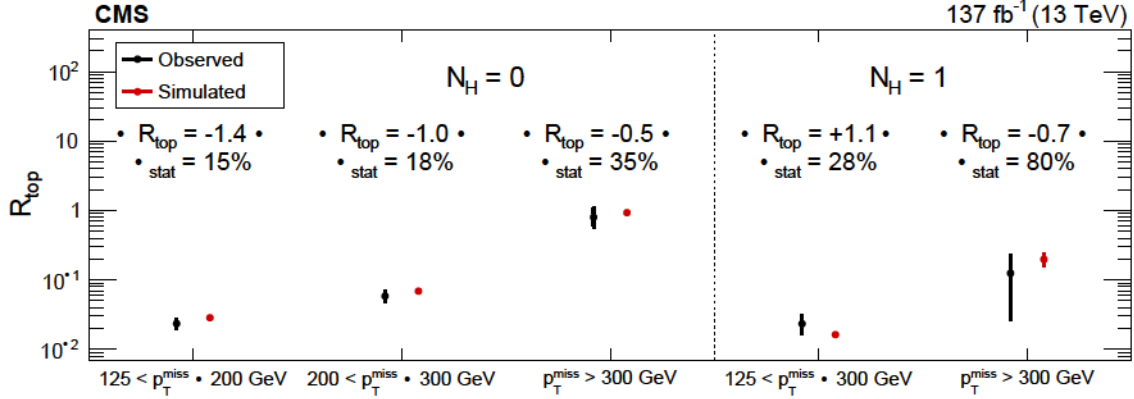


Figure 3: Observed and simulated R_{top} values in the $m_{b\bar{b}} > 150 \text{ GeV}$ validation regions. The differences between observed and simulated R_{top} values, divided by the total statistical uncertainties, are also listed in the figure as ΔR_{top} . The statistical precision of each difference, σ_{stat} , is taken as the systematic uncertainty on R_{top} for the corresponding bin in the signal region.

5.2 W boson background

Events arising from W boson production, mainly W+jets, WW, and WZ, are the second largest background in this search and are the dominant SM contribution in bins with high p_T^{miss} . Events from W+jets production satisfy the baseline selection when they contain true b jets originating from $g \rightarrow b\bar{b}$ (associated W production with heavy-flavor jets, W+HF) or when light-flavor jets are misidentified as b jets (associated W production with light flavor jets, W+LF). Because of the low misidentification rate of light-flavor jets, more than 75% of the selected W+jets events contain at least one genuine b jet. The W+jets background is reduced by the $m_T > 150 \text{ GeV}$ requirement. In absence of large mismeasurements of the p_T^{miss} , the W boson must be produced off-shell in order to satisfy this threshold.

The W boson background is normalized in a data control sample obtained by requiring the number of b-tagged jets (N_b) to be less or equal to 1 and the same m_T , m_{CT} , and $m_{b\bar{b}}$ requirements as the signal regions. The $N_b = 0$ region of this sample is used to normalize the W boson background while the $N_b = 1$ region is used to constrain the contamination from top quark events. The two jets with the highest b tagging discriminator values are used to calculate $m_{b\bar{b}}$ and m_{CT} . The control sample is binned in N_{jets} and p_T^{miss} following the definition of the signal regions and has a high purity of W boson events for $N_b = 0$.

The contribution from processes involving top quarks, mostly single or pair production of top quarks, is up to 20% in some $N_b = 0$ CRs. The contamination is estimated by fitting the N_b distribution in each CR using templates of W+jets and top quark events obtained from simulation. The templates are extracted from simulated W boson and top quark samples, respectively. The number of W boson events in each CR, N_{CR}^W , is obtained by subtracting from the observed

yield, $N_{\text{CR}}^{\text{obs.}}$, the contribution of top quark events $N_{\text{CR}}^{\text{top}}$. For the yield $N_{\text{CR}}^{\text{top}}$, a correction factor obtained from the fit, which is typically close to 1.1, is taken into account.

We define a transfer factor R_W to extrapolate from each $N_b = 0$ CR to the corresponding $N_b = 2$ signal region. Simulated samples of W boson processes are used to calculate R_W . Since there are very few events with an H-tagged large- R jet in the control samples, it is not feasible to form dedicated CRs with $N_H = 1$. Instead, the control samples are inclusive in N_H , and the extrapolation into $N_H = 0$ and $N_H = 1$ is handled by the R_W factors. The predicted yield of the W boson background in each of the signal regions, N_{SR}^W , is therefore given by

$$N_{\text{SR}}^W(p_T^{\text{miss}}, N_{\text{jets}}, N_H) = N_{\text{CR}}^W(p_T^{\text{miss}}, N_{\text{jets}}) R_W(p_T^{\text{miss}}, N_{\text{jets}}, N_H) \quad (5)$$

with

$$N_{\text{CR}}^W(p_T^{\text{miss}}, N_{\text{jets}}) = N_{\text{CR}}^{\text{obs.}}(p_T^{\text{miss}}, N_{\text{jets}}) - N_{\text{CR}}^{\text{top}}(p_T^{\text{miss}}, N_{\text{jets}}), \quad (6)$$

and R_W is defined as

$$R_W(p_T^{\text{miss}}, N_{\text{jets}}, N_H) = \frac{N_{\text{SR}}^{W, \text{MC}}(p_T^{\text{miss}}, N_{\text{jets}}, N_H)}{N_{\text{CR}}^{W, \text{MC}}(p_T^{\text{miss}}, N_{\text{jets}})}. \quad (7)$$

The resulting predictions are shown in Table 6. Section 6 shows a comparison with the observed yields after combining with the other background estimates.

Table 6: The observed ($N_{\text{CR}}^{\text{obs.}}$) and top quark background yield ($N_{\text{CR}}^{\text{top}}$) in the CR, together with the values of R_W for the extrapolation of the W boson background from the CR to the SR, and the final W boson prediction, N_{SR}^W . The uncertainties in R_W include the statistical uncertainty only. The W boson prediction shows both the statistical and systematic uncertainties.

| N_{jets} | p_T^{miss} [GeV] | $N_{\text{CR}}^{\text{obs.}}$ | $N_{\text{CR}}^{\text{top}}$ | | N_{CR}^W | | N_H | R_W | 10^3 | | | N_{SR}^W | |
|-------------------|---------------------------|-------------------------------|------------------------------|-----|-------------------|-----|-------|-------|--------|-----|-----|-------------------|-----|
| 2 | 125–200 | 449 | 65 | 7 | 384 | 23 | 0 | 1.3 | 0.6 | 0.5 | 0.2 | 0.1 | |
| | 200–300 | 314 | 34 | 45 | 280 | 19 | | 3.6 | 0.7 | 1.0 | 0.2 | 0.2 | |
| | 300–400 | 191 | 10 | 1 | 181 | 14 | | 3.7 | 0.7 | 0.7 | 0.1 | 0.1 | |
| | 400 | 110 | 2.5 | 0.7 | 108 | 11 | | 2.8 | 0.8 | 0.3 | 0.1 | 0.1 | |
| | 125–300 | | | | | | 1 | 1.1 | 0.2 | 0.7 | 0.2 | 0.1 | |
| | 300 | | | | | | | 1.7 | 0.7 | 0.5 | 0.2 | 0.2 | |
| | 3 | 125–200 | 329 | 67 | 5 | 262 | 19 | 0 | 0.9 | 0.6 | 0.2 | 0.2 | 0.1 |
| | | 200–300 | 152 | 32 | 5 | 120 | 14 | | 5.9 | 1.5 | 0.7 | 0.2 | 0.1 |
| 300–400 | | 81 | 7 | 1 | 74 | 10 | 9.4 | | 2.6 | 0.7 | 0.2 | 0.2 | |
| 400 | | 44 | 3.7 | 1.7 | 40 | 7 | 6.5 | | 1.9 | 0.3 | 0.1 | 0.1 | |
| 125–300 | | | | | | | 1 | 2.0 | 0.5 | 0.8 | 0.2 | 0.2 | |
| 300 | | | | | | | | 2.9 | 1.7 | 0.3 | 0.2 | 0.1 | |

To assess the modeling of heavy-flavor jets in the simulated W + HF samples, we perform a similar extrapolation in N_b in a Drell–Yan (DY) validation sample assuming $Z \rightarrow \ell\ell$. The large contribution from $t\bar{t}$ in the $N_b = 2$ region is suppressed by requiring two opposite-charge, same-flavor leptons with an invariant mass compatible with a Z boson, $m_{\ell\ell} > m_Z + 5 \text{ GeV}$. In the validation sample, the predicted and observed DY + HF yields agree within 20%. Based on this test, we vary the fraction of W+jets events with at least one generated b jet by 20% and assign the resulting variation of R_W as a systematic uncertainty.

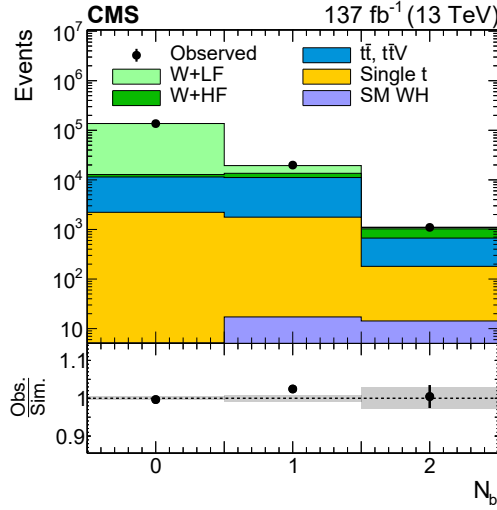


Figure 4: Distribution of N_b in the low- m_T control sample. The $t\bar{t}$ +jets contribution is suppressed by requiring $m_{CT} > 200$ GeV. The shaded area reflects the statistical uncertainty in the simulation.

We also study the distribution of N_b in a low- m_T control sample, obtained by selecting events with $p_T^{\text{miss}} > 125$ GeV, $50 < m_T < 150$ GeV, $N_{\text{jets}} > 2$, and without a requirement on $m_{b\bar{b}}$. The top quark contribution in this region is largely suppressed by the $m_{CT} > 200$ GeV requirement, yielding a sample with a W+HF purity of approximately 40% for $N_b = 2$. Good agreement between data and simulation is observed in this region, as shown in Fig. 4.

Additional contributions to the uncertainty in the factor R_W are evaluated. The difference of the W+HF fraction with respect to the one derived from the DY+HF validation test results in a systematic uncertainty of up to 16% in R_W . Based on the latest measurements [64–66] and considering the delicate phase space requiring significant p_T^{miss} and $N_b = 2$, the diboson production cross section is varied by 25%, yielding a maximum systematic uncertainty of 12%. The uncertainties from the measurement of the b tagging efficiency scale factors are propagated to the simulated W+jets and diboson events resulting in an uncertainty of up to 10% in R_W . The simulated samples are reweighted according to the distribution of the true number of interactions per bunch crossing. The uncertainty in the total inelastic pp cross section results in uncertainties of 2–6% in R_W . The uncertainty arising from the jet energy calibration [67] is assessed by shifting jet momenta in simulated samples up and down, and propagating the resulting changes to R_W . Typical values for the systematic uncertainty from the jet energy scale range from 2–10%, reaching up to 20% for events with a boosted Higgs boson candidate.

The mistag rate of the H tagging algorithm for large- R jets that do not contain a true H is measured in a control sample obtained by requiring low- m_T , $N_b = 2$, and at least one large- R jet. Scale factors are measured and applied to simulation to correct for differences in the observed mistag rates. The uncertainty in the scale factors is dominated by the limited statistical precision of the control sample and results in a systematic uncertainty up to 14% in R_W .

The renormalization (μ_R) and factorization (μ_F) scales are varied up and down by a factor of 2, omitting the combination of variations in opposite directions. The envelope of the variations reaches values up to 15% and is assigned as systematic uncertainty. The uncertainties resulting from variations of the PDF and the strong coupling α_s are less than 2%. The systematic uncertainties in R_W are summarized in Table 7.

Table 7: Systematic uncertainties on R_W .

| Source | Typical values |
|-----------------------|----------------|
| W HF fraction | 7–16% |
| Diboson cross section | 1–12% |
| b tagging efficiency | 3–10% |
| H mistag rate | 3–14% |
| Jet energy scale | 2–20% |
| Pileup | 1–6% |
| PDF | 2% |
| S | 2% |
| R and F | 3–15% |

6 Results and interpretation

The observed data yields and the expected yields from SM processes in the signal regions are summarized in Table 8. No significant disagreement is observed. A binned maximum likelihood fit for the SUSY signal strength, the yields of background events, and various nuisance parameters is performed. The likelihood function is built using Poisson probability functions for all signal regions, and log-normal or gamma function PDFs for all nuisance parameters. Figure 5 shows the post-fit expectation of the SM background. Combining all signal bins, 51 \pm 5 background events are expected and 49 events are observed.

Table 8: Summary of the predicted SM background and the observed yield in the signal regions, together with the expected yields for three signal benchmark models. The total prediction, $N_{\text{SR}}^{\text{BG}}$, is the sum of the top quark and W boson predictions, $N_{\text{SR}}^{\text{top}}$ and N_{SR}^{W} , as well as small contributions from standard model WH production. The values shown are taken before the signal extraction fit to the observed yields in the signal regions is performed. The uncertainties include the statistical and systematic components. For each benchmark model column, the ordered pairs indicate the masses (in GeV) of the $\tilde{0}/\tilde{1}$ and $\tilde{0}'/\tilde{1}'$, respectively.

| N_{jets} | N_{H} | $p_{\text{T}}^{\text{miss}}$ [GeV] | $N_{\text{SR}}^{\text{top}}$ | N_{SR}^{W} | $N_{\text{SR}}^{\text{BG}}$ | Observed | $\tilde{0}/\tilde{1}$ 800, 100 | H $\tilde{0}'/\tilde{1}'$ 425, 150 | W $\tilde{0}/\tilde{1}$ 225, 75 | | | | |
|-------------------|----------------|------------------------------------|------------------------------|----------------------------|-----------------------------|----------|-----------------------------------|---------------------------------------|------------------------------------|-----|-----|------|------|
| 2 | 0 | 125–200 | 6.3 | 0.5 | 6.9 | 1.3 | 8 | 0.08 | 0.02 | 2.0 | 0.4 | 2.6 | 0.8 |
| | | 200–300 | 2.4 | 1.0 | 3.4 | 0.6 | 2 | 0.3 | 0.1 | 4.5 | 0.7 | 2.9 | 0.6 |
| | | 300–400 | 0.3 | 0.7 | 1.0 | 0.3 | 1 | 0.3 | 0.1 | 2.1 | 0.4 | 0.3 | 0.2 |
| | | 400 | 0.02 | 0.3 | 0.3 | 0.1 | 1 | 0.5 | 0.2 | 0.4 | 0.3 | 0.01 | |
| | 1 | 125–300 | 1.6 | 0.7 | 2.5 | 0.9 | 3 | 0.5 | 0.1 | 3.9 | 0.7 | 2.8 | 1.0 |
| | | 300 | 0.4 | 0.5 | 0.9 | 0.5 | 1 | 2.6 | 0.4 | 4.3 | 0.8 | 1.4 | 0.4 |
| 3 | 0 | 125–200 | 17.5 | 0.2 | 17.8 | 3.0 | 17 | 0.05 | 0.02 | 1.0 | 0.2 | 2.9 | 0.6 |
| | | 200–300 | 7.1 | 0.7 | 7.8 | 1.7 | 6 | 0.14 | 0.03 | 2.6 | 0.3 | 2.1 | 0.5 |
| | | 300–400 | 0.8 | 0.7 | 1.5 | 0.5 | 0 | 0.18 | 0.04 | 1.2 | 0.4 | 0.4 | 0.4 |
| | | 400 | 0.2 | 0.3 | 0.5 | 0.3 | 0 | 0.3 | 0.1 | 0.3 | 0.2 | 0.06 | 0.06 |
| | 1 | 125–300 | 5.0 | 0.8 | 5.9 | 2.1 | 10 | 0.4 | 0.1 | 2.6 | 0.5 | 2.0 | 0.6 |
| | | 300 | 1.7 | 0.3 | 2.1 | 1.6 | 0 | 1.5 | 0.2 | 2.4 | 0.5 | 0.6 | 0.2 |

We next evaluate the experimental and theoretical uncertainties in the expected signal yield. Varying the lepton, b tagging, and H tagging efficiency scale factors by their respective uncertainties varies the signal yield by less than 1, 4, and 20%. For the H tagger, this scale factor is measured as a function of the H candidate p_{T} using a sample of jets in data and simulation that mimic the rare H \rightarrow $b\bar{b}$ case [60].

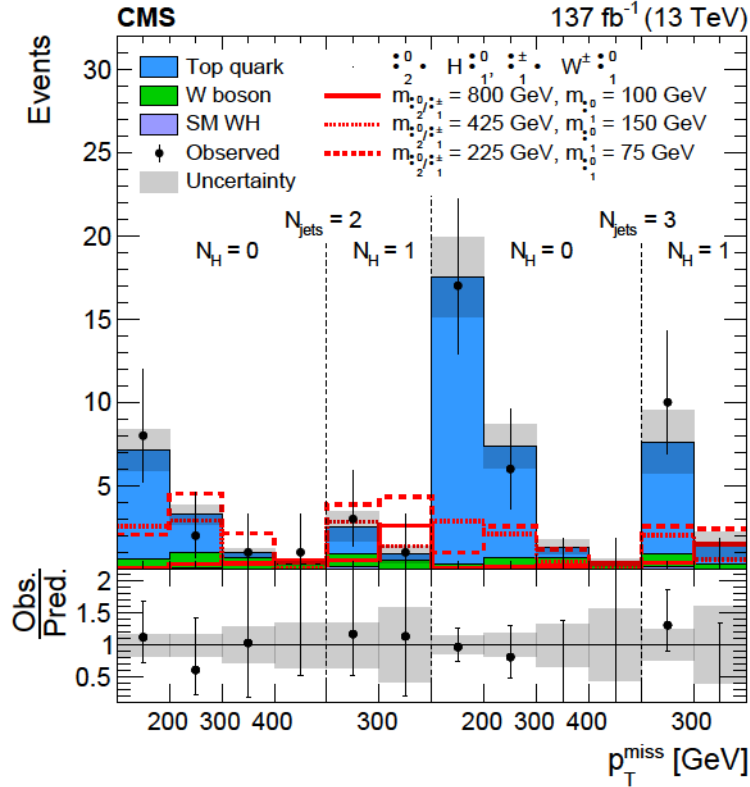


Figure 5: Predictions of the SM background after performing the signal extraction fit (filled histograms) and observed yields in the signal regions. Three signal models with different values of $m_{\tilde{\chi}_2^0/\tilde{\chi}_1^\pm}$ and $m_{\tilde{\chi}_1^0}$ are shown as solid, short dashed, and long dashed lines. The lower panel provides the ratio between the observation and the predicted SM backgrounds. The shaded band shows the post-fit combination of the systematic and statistical uncertainties in the background prediction.

The efficiencies obtained using the fast or full detector simulation are found to be compatible, with no significant dependence on the mass splitting $\Delta m = m_{\tilde{\chi}_2^0/\tilde{\chi}_1^\pm} - m_{\tilde{\chi}_1^0}$. The systematic uncertainty in the signal yields, due to the uncertainty in the trigger efficiency measurement, is generally less than 5%.

The uncertainties in the simulated yields obtained by varying the jet energy scale and the jet energy resolution are each between 1 and 7%. A 3% difference in the b jet energy scale between the fast and full detector simulations is observed, resulting in a 1–10% change in the expected signal yield.

The effect of missing higher-order corrections on the signal acceptance is estimated by varying μ_R and μ_F [68–70] up and down by a factor of 2, omitting the combination of variations in opposite directions. The envelope of the variations reaches values up to 15% and is assigned as a systematic uncertainty. The resulting variation of the expected signal yield is less than 1%. To account for uncertainty in the modeling of the multiplicity of additional jets from initial state radiation, a 1% uncertainty is applied to the $N_{\text{jets}} = 3$ signal regions.

The integrated luminosities of the 2016, 2017, and 2018 data-taking periods are individually known with uncertainties in the 2.3–2.5% range [71–73], while the total Run 2 (2016–2018) integrated luminosity has an uncertainty of 1.8%, the improvement in precision reflecting the

Table 9: Sources and ranges of systematic uncertainties on the expected signal yields. The ranges reported reflect the magnitudes of the median 68% of all impacts, considering the distribution of variations in all 12 signal regions and the full range of signal mass hypotheses used. When the lower bound is very close to 0, an upper bound is shown instead.

| Source | Typical values |
|------------------------------------|----------------|
| Simulation statistical uncertainty | 1–10% |
| Lepton efficiency | 1% |
| b tagging efficiency | 4% |
| H tagging efficiency | 7–20% |
| Trigger efficiency | 5% |
| Jet energy scale | 1–7% |
| Jet energy resolution | 1–7% |
| b jet energy scale | 1–10% |
| R and F | 1% |
| Initial-state radiation | 1% |
| Integrated luminosity | 1.8% |
| Pileup | 2% |

(uncorrelated) time evolution of some systematic effects. The signal samples are reweighted according to the distribution of the true number of interactions per bunch crossing. The uncertainty in the total inelastic pp cross section leads to changes in the expected signal yield of less than 2%. A summary of the systematic uncertainties in the signal yields is given in Table 9.

The results are interpreted in the context of the simplified SUSY model shown in Fig. 1. The chargino and second-lightest neutralino are assumed to have the same mass, and the branching fractions for the decays shown are taken to be 100%. Wino-like cross sections are assumed. Cross section limits as a function of the masses of the produced particles are set using a modified frequentist approach at 95% confidence level (CL), with the CL_s criterion and an asymptotic formulation [74–76]. All signal regions are considered simultaneously and correlations among uncertainties are included.

Figure 6 shows the 95% CL upper limits on the cross section, together with the expected and observed exclusion limits in the $m_{\tilde{\chi}_1^0} - m_{\tilde{\chi}_2^0}$ plane for chargino-neutralino production.

This analysis excludes charginos with mass below 820 GeV for a low-mass LSP, and values of the LSP mass up to approximately 350 GeV for a chargino mass near 700 GeV. The excluded cross section for models with large mass splitting reaches approximately 5 fb.

7 Summary

This paper presents the results of a search for chargino-neutralino production in a final state containing a W boson decaying to leptons, a Higgs boson decaying to a bottom quark-antiquark pair, and missing transverse momentum. Expected yields from standard model processes are estimated by extrapolating the yields observed in control regions using transfer factors obtained from simulation. The observed yields agree with those expected from the standard model. The results are interpreted as an exclusion of a simplified model of chargino-neutralino production. In the simplified model, the chargino decays to a W boson and a lightest supersymmetric particle (LSP), and the next-to-lightest neutralino decays to a Higgs boson and an LSP. Charginos with mass below 820 GeV are excluded at 95% confidence level for an LSP with mass below 200 GeV, and values of LSP mass up to approximately 350 GeV are excluded

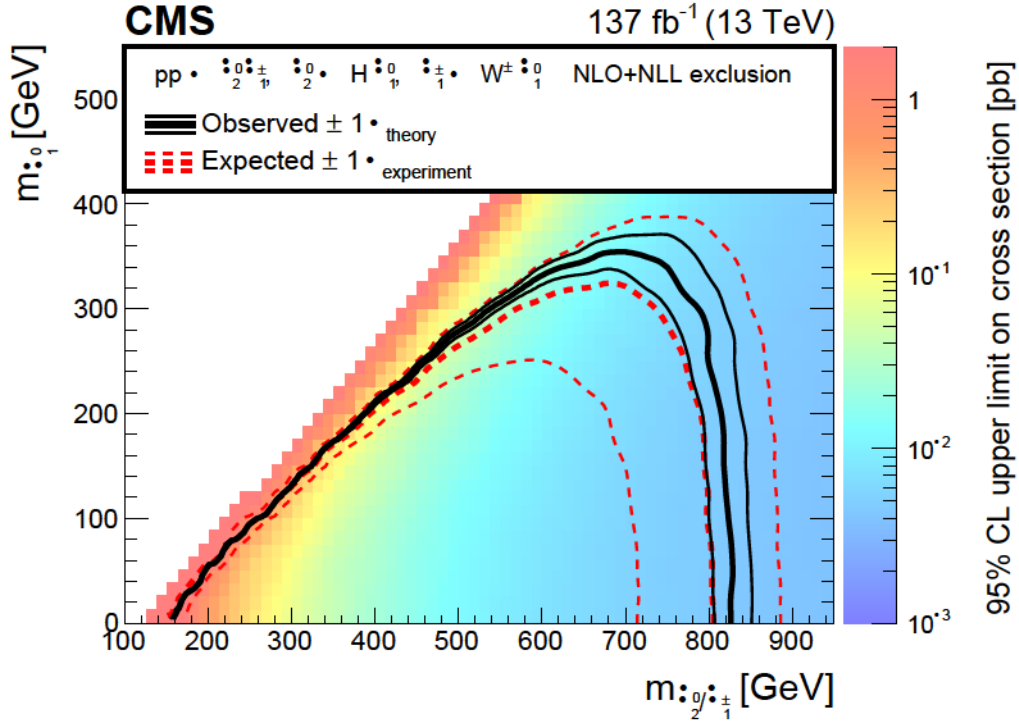


Figure 6: Cross section upper limits calculated with the background estimates and all of the background systematic uncertainties described in Sections 5.1 and 5.2. The color on the z axis represents the 95% CL upper limit on the cross section calculated at each point in the $m_{\tilde{\chi}_1^0}$ - $m_{\tilde{\chi}_2^0}$ plane. The area below the thick black curve (dashed red line) represents the observed (expected) exclusion region at this CL. The region containing 68% of the distribution of limits expected under the background-only hypothesis is bounded by thin dashed red lines. The thin black lines show the effect of the theoretical uncertainties in the signal cross section.

for a chargino mass near 700 GeV.

Relative to the previous result from the CMS Collaboration targeting this signature [12], the sensitivity of the search has been significantly extended. The constraints on the masses of the chargino and LSP exceed those from the previous analysis by nearly 350 and 250 GeV, respectively. This represents a factor of 14 reduction in the excluded cross section for models with large mass splittings. Roughly half of this improvement is the result of the four-fold increase in integrated luminosity, with the remainder coming from analysis optimizations such as the inclusion of the H tagger and events with $N_{\text{jets}} = 3$, as well as finer categorization of events based on $p_{\text{T}}^{\text{miss}}$ made possible by the increased size of the data set.

Acknowledgments

We congratulate our colleagues in the CERN accelerator departments for the excellent performance of the LHC and thank the technical and administrative staffs at CERN and at other CMS institutes for their contributions to the success of the CMS effort. In addition, we gratefully acknowledge the computing centers and personnel of the Worldwide LHC Computing Grid and other centers for delivering so effectively the computing infrastructure essential to our analyses. Finally, we acknowledge the enduring support for the construction and operation

of the LHC, the CMS detector, and the supporting computing infrastructure provided by the following funding agencies: BMBWF and FWF (Austria); FNRS and FWO (Belgium); CNPq, CAPES, FAPERJ, FAPERGS, and FAPESP (Brazil); MES (Bulgaria); CERN; CAS, MoST, and NSFC (China); MINCIENCIAS (Colombia); MSES and CSF (Croatia); RIF (Cyprus); SENESCYT (Ecuador); MoER, ERC PUT and ERDF (Estonia); Academy of Finland, MEC, and HIP (Finland); CEA and CNRS/IN2P3 (France); BMBF, DFG, and HGF (Germany); GSRT (Greece); NKFI (Hungary); DAE and DST (India); IPM (Iran); SFI (Ireland); INFN (Italy); MSIP and NRF (Republic of Korea); MES (Latvia); LAS (Lithuania); MOE and UM (Malaysia); BUAP, CINVESTAV, CONACYT, LNS, SEP, and UASLP-FAI (Mexico); MOS (Montenegro); MBIE (New Zealand); PAEC (Pakistan); MSHE and NSC (Poland); FCT (Portugal); JINR (Dubna); MON, RosAtom, RAS, RFBR, and NRC KI (Russia); MESTD (Serbia); SEIDI, CPAN, PCTI, and FEDER (Spain); MOSTR (Sri Lanka); Swiss Funding Agencies (Switzerland); MST (Taipei); ThEP Center, IPST, STAR, and NSTDA (Thailand); TUBITAK and TAEK (Turkey); NASU (Ukraine); STFC (United Kingdom); DOE and NSF (USA).

Individuals have received support from the Marie-Curie program and the European Research Council and Horizon 2020 Grant, contract Nos. 675440, 724704, 752730, 758316, 765710, 824093, and COST Action CA16108 (European Union); the Leventis Foundation; the Alfred P. Sloan Foundation; the Alexander von Humboldt Foundation; the Belgian Federal Science Policy Office; the Fonds pour la Formation à la Recherche dans l'Industrie et dans l'Agriculture (FRIA-Belgium); the Agentschap voor Innovatie door Wetenschap en Technologie (IWT-Belgium); the F.R.S.-FNRS and FWO (Belgium) under the "Excellence of Science – EOS" – be.h project n. 30820817; the Beijing Municipal Science & Technology Commission, No. Z191100007219010; the Ministry of Education, Youth and Sports (MEYS) of the Czech Republic; the Deutsche Forschungsgemeinschaft (DFG), under Germany's Excellence Strategy – EXC 2121 "Quantum Universe" – 390833306, and under project number 400140256 - GRK2497; the Lendület ("Momentum") Program and the János Bolyai Research Scholarship of the Hungarian Academy of Sciences, the New National Excellence Program ÚNKP, the NKFI research grants 123842, 123959, 124845, 124850, 125105, 128713, 128786, and 129058 (Hungary); the Council of Science and Industrial Research, India; the Latvian Council of Science; the Ministry of Science and Higher Education and the National Science Center, contracts Opus 2014/15/B/ST2/03998 and 2015/19/B/ST2/02861 (Poland); the National Priorities Research Program by Qatar National Research Fund; the Ministry of Science and Higher Education, project no. 0723-2020-0041 (Russia); the Programa Estatal de Fomento de la Investigación Científica y Técnica de Excelencia María de Maeztu, grant MDM-2015-0509 and the Programa Severo Ochoa del Principado de Asturias; the Stavros Niarchos Foundation (Greece); the Rachadapisek Sompot Fund for Postdoctoral Fellowship, Chulalongkorn University and the Chulalongkorn Academic into Its 2nd Century Project Advancement Project (Thailand); the Kavli Foundation; the Nvidia Corporation; the SuperMicro Corporation; the Welch Foundation, contract C-1845; and the Weston Havens Foundation (USA).

References

- [1] P. Ramond, "Dual theory for free fermions", *Phys. Rev. D* **3** (1971) 2415, doi:10.1103/PhysRevD.3.2415.
- [2] J. Wess and B. Zumino, "Supergauge transformations in four dimensions", *Nucl. Phys. B* **70** (1974) 39, doi:10.1016/0550-3213(74)90355-1.

-
- [3] H. P. Nilles, “Supersymmetry, supergravity and particle physics”, *Phys. Rept.* **110** (1984) 1, doi:10.1016/0370-1573(84)90008-5.
- [4] B. de Carlos and J. A. Casas, “One-loop analysis of the electroweak breaking in supersymmetric models and the fine tuning problem”, *Phys. Lett. B* **309** (1993) 320, doi:10.1016/0370-2693(93)90940-J, arXiv:hep-ph/9303291.
- [5] S. Dimopoulos and G. F. Giudice, “Naturalness constraints in supersymmetric theories with nonuniversal soft terms”, *Phys. Lett. B* **357** (1995) 573, doi:10.1016/0370-2693(95)00961-J, arXiv:hep-ph/9507282.
- [6] G. R. Farrar and P. Fayet, “Phenomenology of the production, decay, and detection of new hadronic states associated with supersymmetry”, *Phys. Lett. B* **76** (1978) 575, doi:10.1016/0370-2693(78)90858-4.
- [7] J. Alwall, P. Schuster, and N. Toro, “Simplified models for a first characterization of new physics at the LHC”, *Phys. Rev. D* **79** (2009) 075020, doi:10.1103/PhysRevD.79.075020, arXiv:0810.3921.
- [8] LHC New Physics Working Group, “Simplified models for LHC new physics searches”, *J. Phys. G* **39** (2012) 105005, doi:10.1088/0954-3899/39/10/105005, arXiv:1105.2838.
- [9] CMS Collaboration, “Interpretation of searches for supersymmetry with simplified models”, *Phys. Rev. D* **88** (2013) 052017, doi:10.1103/PhysRevD.88.052017, arXiv:1301.2175.
- [10] ATLAS Collaboration, “Search for direct production of electroweakinos in final states with one lepton, missing transverse momentum and a Higgs boson decaying into two b-jets in pp collisions $\sqrt{s} = 13$ TeV with the ATLAS detector”, *Eur. Phys. J. C* **80** (2020) 691, doi:10.1140/epjc/s10052-020-8050-3, arXiv:1909.09226.
- [11] ATLAS Collaboration, “Search for the electroweak production of supersymmetric particles in $\sqrt{s} = 8$ TeV pp collisions with the ATLAS detector”, *Phys. Rev. D* **93** (2016) 052002, doi:10.1103/PhysRevD.93.052002, arXiv:1509.07152.
- [12] CMS Collaboration, “Search for electroweak production of charginos and neutralinos in WH events in proton-proton collisions at $\sqrt{s} = 13$ TeV”, *JHEP* **11** (2017) 029, doi:10.1007/JHEP11(2017)029, arXiv:1706.09933.
- [13] CMS Collaboration, “Searches for electroweak neutralino and chargino production in channels with Higgs, Z, and W bosons in pp collisions at 8 TeV”, *Phys. Rev. D* **90** (2014) 092007, doi:10.1103/PhysRevD.90.092007, arXiv:1409.3168.
- [14] CMS Collaboration, “Searches for electroweak production of charginos, neutralinos, and sleptons decaying to leptons and W, Z, and Higgs bosons in pp collisions at 8 TeV”, *Eur. Phys. J. C* **74** (2014) 3036, doi:10.1140/epjc/s10052-014-3036-7, arXiv:1405.7570.
- [15] CMS Collaboration, “The CMS experiment at the CERN LHC”, *JINST* **3** (2008) S08004, doi:10.1088/1748-0221/3/08/S08004.
- [16] CMS Collaboration, “Performance of the CMS Level-1 trigger in proton-proton collisions at $\sqrt{s} = 13$ TeV”, *JINST* **15** (2020) P10017, doi:10.1088/1748-0221/15/10/P10017, arXiv:2006.10165.

- [17] CMS Collaboration, “The CMS trigger system”, *JINST* **12** (2017) P01020, doi:10.1088/1748-0221/12/01/P01020, arXiv:1609.02366.
- [18] J. Alwall et al., “The automated computation of tree-level and next-to-leading order differential cross sections, and their matching to parton shower simulations”, *JHEP* **07** (2014) 079, doi:10.1007/JHEP07(2014)079, arXiv:1405.0301.
- [19] P. Nason, “A new method for combining NLO QCD with shower Monte Carlo algorithms”, *JHEP* **11** (2004) 040, doi:10.1088/1126-6708/2004/11/040, arXiv:hep-ph/0409146.
- [20] S. Frixione, P. Nason, and C. Oleari, “Matching NLO QCD computations with parton shower simulations: the POWHEG method”, *JHEP* **11** (2007) 070, doi:10.1088/1126-6708/2007/11/070, arXiv:0709.2092.
- [21] S. Alioli, P. Nason, C. Oleari, and E. Re, “A general framework for implementing NLO calculations in shower Monte Carlo programs: the POWHEG BOX”, *JHEP* **06** (2010) 043, doi:10.1007/JHEP06(2010)043, arXiv:1002.2581.
- [22] E. Re, “Single-top Wt -channel production matched with parton showers using the POWHEG method”, *Eur. Phys. J. C* **71** (2011) 1547, doi:10.1140/epjc/s10052-011-1547-z, arXiv:1009.2450.
- [23] NNPDF Collaboration, “Unbiased global determination of parton distributions and their uncertainties at NNLO and at LO”, *Nucl. Phys. B* **855** (2012) 153, doi:10.1016/j.nuclphysb.2011.09.024, arXiv:1107.2652.
- [24] NNPDF Collaboration, “Parton distributions for the LHC Run II”, *JHEP* **04** (2015) 040, doi:10.1007/JHEP04(2015)040, arXiv:1410.8849.
- [25] NNPDF Collaboration, “Parton distributions from high-precision collider data”, *Eur. Phys. J. C* **77** (2017) 663, doi:10.1140/epjc/s10052-017-5199-5, arXiv:1706.00428.
- [26] T. Sjöstrand et al., “An introduction to PYTHIA 8.2”, *Comput. Phys. Commun.* **191** (2015) 159, doi:10.1016/j.cpc.2015.01.024, arXiv:1410.3012.
- [27] J. Alwall et al., “Comparative study of various algorithms for the merging of parton showers and matrix elements in hadronic collisions”, *Eur. Phys. J. C* **53** (2008) 473, doi:10.1140/epjc/s10052-007-0490-5, arXiv:0706.2569.
- [28] R. Frederix and S. Frixione, “Merging meets matching in MC@NLO”, *JHEP* **12** (2012) 061, doi:10.1007/JHEP12(2012)061, arXiv:1209.6215.
- [29] CMS Collaboration, “Event generator tunes obtained from underlying event and multiparton scattering measurements”, *Eur. Phys. J. C* **76** (2016) 155, doi:10.1140/epjc/s10052-016-3988-x, arXiv:1512.00815.
- [30] CMS Collaboration, “Extraction and validation of a new set of CMS PYTHIA8 tunes from underlying-event measurements”, *Eur. Phys. J. C* **80** (2020) 4, doi:10.1140/epjc/s10052-019-7499-4, arXiv:1903.12179.
- [31] GEANT4 Collaboration, “GEANT4 — a simulation toolkit”, *Nucl. Instrum. Meth. A* **506** (2003) 250, doi:10.1016/S0168-9002(03)01368-8.

-
- [32] S. Abdullin et al., “The fast simulation of the CMS detector at LHC”, *J. Phys. Conf. Ser.* **331** (2011) 032049, doi:10.1088/1742-6596/331/3/032049.
- [33] A. Giammanco, “The fast simulation of the CMS experiment”, *J. Phys. Conf. Ser.* **513** (2014) 022012, doi:10.1088/1742-6596/513/2/022012.
- [34] Y. Li and F. Petriello, “Combining QCD and electroweak corrections to dilepton production in FEWZ”, *Phys. Rev. D* **86** (2012) 094034, doi:10.1103/PhysRevD.86.094034, arXiv:1208.5967.
- [35] M. Aliev et al., “HATHOR: HAdronic Top and Heavy quarks crOss section calculator”, *Comput. Phys. Commun.* **182** (2011) 1034, doi:10.1016/j.cpc.2010.12.040, arXiv:1007.1327.
- [36] P. Kant et al., “HatHor for single top-quark production: Updated predictions and uncertainty estimates for single top-quark production in hadronic collisions”, *Comput. Phys. Commun.* **191** (2015) 74, doi:10.1016/j.cpc.2015.02.001, arXiv:1406.4403.
- [37] M. Beneke, P. Falgari, S. Klein, and C. Schwinn, “Hadronic top-quark pair production with NNLL threshold resummation”, *Nucl. Phys. B* **855** (2012) 695, doi:10.1016/j.nuclphysb.2011.10.021, arXiv:1109.1536.
- [38] M. Cacciari et al., “Top-pair production at hadron colliders with next-to-next-to-leading logarithmic soft-gluon resummation”, *Phys. Lett. B* **710** (2012) 612, doi:10.1016/j.physletb.2012.03.013, arXiv:1111.5869.
- [39] M. Czakon and A. Mitov, “Top++: A program for the calculation of the top-pair cross-section at hadron colliders”, *Comput. Phys. Commun.* **185** (2014) 2930, doi:10.1016/j.cpc.2014.06.021, arXiv:1112.5675.
- [40] P. Bärnreuther, M. Czakon, and A. Mitov, “Percent level precision physics at the Tevatron: First genuine NNLO QCD corrections to $q\bar{q} \rightarrow t\bar{t} X$ ”, *Phys. Rev. Lett.* **109** (2012) 132001, doi:10.1103/PhysRevLett.109.132001, arXiv:1204.5201.
- [41] M. Czakon and A. Mitov, “NNLO corrections to top-pair production at hadron colliders: the all-fermionic scattering channels”, *JHEP* **12** (2012) 054, doi:10.1007/JHEP12(2012)054, arXiv:1207.0236.
- [42] M. Czakon and A. Mitov, “NNLO corrections to top pair production at hadron colliders: the quark-gluon reaction”, *JHEP* **01** (2013) 080, doi:10.1007/JHEP01(2013)080, arXiv:1210.6832.
- [43] M. Czakon, P. Fiedler, and A. Mitov, “Total top-quark pair-production cross section at hadron colliders through $O(\frac{4}{s})$ ”, *Phys. Rev. Lett.* **110** (2013) 252004, doi:10.1103/PhysRevLett.110.252004, arXiv:1303.6254.
- [44] W. Beenakker, M. Klasen, and Kr “Production of charginos, neutralinos, and sleptons at hadron colliders”,.
- [45] J. Debove, B. Fuks, and M. Klasen, “Threshold resummation for gaugino pair production at hadron colliders”, *Nuc. Phys. B* **842** (2011) doi:10.1016/j.nuclphysb.2010.08.016, arXiv:1005.2909.

- [46] B. Fuks, M. Klasen, D. R. Lamprea, and M. Rothering, “Precision predictions for electroweak superpartner production at hadron colliders with resumino”, *Eur. Phys. J. C* **73** (2013) 2480, doi:10.1140/epjc/s10052-013-2480-0, arXiv:1304.0790.
- [47] J. Fiaschi and M. Klasen, “Neutralino-chargino pair production at NLO+NLL with resummation-improved parton density functions for LHC Run II”, *Phys. Rev. D* **98** (2018) 055014, doi:10.1103/PhysRevD.98.055014, arXiv:1805.11322.
- [48] LHC Higgs Cross Section Working Group, “Handbook of LHC Higgs cross sections: 4. Deciphering the nature of the Higgs sector”, CERN Report CERN-2017-002-M, 2016. doi:10.23731/CYRM-2017-002, arXiv:1610.07922.
- [49] CMS Collaboration, “Search for direct top squark pair production in events with one lepton, jets, and missing transverse momentum at 13 TeV with the CMS experiment”, *JHEP* **05** (2020) 032, doi:10.1007/jhep05(2020)032, arXiv:1912.08887.
- [50] CMS Collaboration, “Particle-flow reconstruction and global event description with the CMS detector”, *JINST* **12** (2017) P10003, doi:10.1088/1748-0221/12/10/P10003, arXiv:1706.04965.
- [51] CMS Collaboration, “Performance of missing transverse momentum reconstruction in proton-proton collisions at \sqrt{s} 13 TeV using the CMS detector”, *JINST* **14** (2019) P07004, doi:10.1088/1748-0221/14/07/P07004, arXiv:1903.06078.
- [52] CMS Collaboration, “Electron and photon reconstruction and identification with the CMS experiment at the CERN LHC”, *JINST* **16** (2021) P05014, doi:10.1088/1748-0221/16/05/p05014, arXiv:2012.06888.
- [53] CMS Collaboration, “Performance of the CMS muon detector and muon reconstruction with proton-proton collisions at \sqrt{s} 13 TeV”, *JINST* **13** (2018) P06015, doi:10.1088/1748-0221/13/06/P06015, arXiv:1804.04528.
- [54] CMS Collaboration, “Reconstruction and identification of τ lepton decays to hadrons and ν_τ at CMS”, *JINST* **11** (2016) P01019, doi:10.1088/1748-0221/11/01/P01019, arXiv:1510.07488.
- [55] CMS Collaboration, “Performance of reconstruction and identification of τ leptons decaying to hadrons and ν_τ in pp collisions at \sqrt{s} 13 TeV”, *JINST* **13** (2018) P10005, doi:10.1088/1748-0221/13/10/p10005, arXiv:1809.02816.
- [56] M. Cacciari, G. P. Salam, and G. Soyez, “The anti- k_T jet clustering algorithm”, *JHEP* **04** (2008) 063, doi:10.1088/1126-6708/2008/04/063, arXiv:0802.1189.
- [57] M. Cacciari, G. P. Salam, and G. Soyez, “FastJet user manual”, *Eur. Phys. J. C* **72** (2012) 1896, doi:10.1140/epjc/s10052-012-1896-2, arXiv:1111.6097.
- [58] CMS Collaboration, “Determination of jet energy calibration and transverse momentum resolution in CMS”, *JINST* **6** (2011) P11002, doi:10.1088/1748-0221/6/11/P11002, arXiv:1107.4277.
- [59] CMS Collaboration, “Identification of heavy-flavour jets with the CMS detector in pp collisions at 13 TeV”, *JINST* **13** (2018) P05011, doi:10.1088/1748-0221/13/05/P05011, arXiv:1712.07158.

-
- [60] CMS Collaboration, “Identification of heavy, energetic, hadronically decaying particles using machine-learning techniques”, *JINST* **15** (2020) P06005, doi:10.1088/1748-0221/15/06/P06005, arXiv:2004.08262.
- [61] CMS Collaboration, “Missing transverse energy performance of the CMS detector”, *JINST* **6** (2011) P09001, doi:10.1088/1748-0221/6/09/P09001, arXiv:1106.5048.
- [62] D. R. Tovey, “On measuring the masses of pair-produced semi-invisibly decaying particles at hadron colliders”, *JHEP* **04** (2008) 034, doi:10.1088/1126-6708/2008/04/034, arXiv:0802.2879.
- [63] CMS Collaboration, “Observation of Higgs boson decay to bottom quarks”, *Phys. Rev. Lett.* **121** (2018) 121801, doi:10.1103/PhysRevLett.121.121801, arXiv:1808.08242.
- [64] CMS Collaboration, “Measurements of the $pp \rightarrow WZ$ inclusive and differential production cross section and constraints on charged anomalous triple gauge couplings at $\sqrt{s} = 13$ TeV”, *JHEP* **04** (2019) 122, doi:10.1007/JHEP04(2019)122, arXiv:1901.03428.
- [65] CMS Collaboration, “ W^+W^- boson pair production in proton-proton collisions at $\sqrt{s} = 13$ TeV”, *Phys. Rev. D* **102** (2020) 092001, doi:10.1103/PhysRevD.102.092001, arXiv:2009.00119.
- [66] CMS Collaboration, “Measurements of $pp \rightarrow ZZ$ production cross sections and constraints on anomalous triple gauge couplings at $\sqrt{s} = 13$ TeV”, *Eur. Phys. J. C* **81** (2021) 200, doi:10.1140/epjc/s10052-020-08817-8, arXiv:2009.01186.
- [67] CMS Collaboration, “Jet energy scale and resolution performance with 13 TeV data collected by CMS in 2016-2018”, CMS Detector Performance Summary, CMS-DP-2020-019, 2020.
- [68] S. Catani, D. de Florian, M. Grazzini, and P. Nason, “Soft gluon resummation for Higgs boson production at hadron colliders”, *JHEP* **07** (2003) 028, doi:10.1088/1126-6708/2003/07/028, arXiv:hep-ph/0306211.
- [69] M. Cacciari et al., “The $t\bar{t}$ cross-section at 1.8 TeV and 1.96 TeV: A study of the systematics due to parton densities and scale dependence”, *JHEP* **04** (2004) 068, doi:10.1088/1126-6708/2004/04/068, arXiv:hep-ph/0303085.
- [70] A. Kalogeropoulos and J. Alwall, “The SysCalc code: A tool to derive theoretical systematic uncertainties”, 2018. arXiv:1801.08401.
- [71] CMS Collaboration, “CMS luminosity measurements for the 2016 data-taking period”, CMS Physics Analysis Summary, CMS-PAS-LUM-17-001, 2017.
- [72] CMS Collaboration, “CMS luminosity measurement for the 2017 data-taking period at $\sqrt{s} = 13$ TeV”, CMS Physics Analysis Summary, CMS-PAS-LUM-17-004, 2018.
- [73] CMS Collaboration, “CMS luminosity measurement for the 2018 data-taking period at $\sqrt{s} = 13$ TeV”, CMS Physics Analysis Summary, CMS-PAS-LUM-18-002, 2019.
- [74] T. Junk, “Confidence level computation for combining searches with small statistics”, *Nucl. Instrum. Meth. A* **434** (1999) 435, doi:10.1016/S0168-9002(99)00498-2.

-
- [75] A. L. Read, "Presentation of search results: the CL_s technique", *J. Phys. G* **28** (2002) 2693, doi:10.1088/0954-3899/28/10/313.
- [76] G. Cowan, K. Cranmer, E. Gross, and O. Vitells, "Asymptotic formulae for likelihood-based tests of new physics", *Eur. Phys. J. C* **71** (2011) 1554, doi:10.1140/epjc/s10052-011-1554-0, arXiv:1007.1727. [Erratum: doi:10.1140/epjc/s10052-013-2501-z].

A The CMS Collaboration

Yerevan Physics Institute, Yerevan, Armenia

A. Tumasyan

Institut für Hochenergiephysik, Wien, Austria

W. Adam, J.W. Andrejkovic, T. Bergauer, S. Chatterjee, M. Dragicevic, A. Escalante Del Valle, R. Frühwirth¹, M. Jeitler¹, N. Krammer, L. Lechner, D. Liko, I. Mikulec, P. Paulitsch, F.M. Pitters, J. Schieck¹, R. Schöfbeck, M. Spanring, S. Templ, W. Waltenberger, C.-E. Wulz¹

Institute for Nuclear Problems, Minsk, Belarus

V. Chekhovsky, A. Litomin, V. Makarenko

Universiteit Antwerpen, Antwerpen, Belgium

M.R. Darwish², E.A. De Wolf, X. Janssen, T. Kello³, A. Lelek, H. Rejeb Sfar, P. Van Mechelen, S. Van Putte, N. Van Remortel

Vrije Universiteit Brussel, Brussel, Belgium

F. Blekman, E.S. Bols, J. D'Hondt, J. De Clercq, M. Delcourt, H. El Faham, S. Lowette, S. Moortgat, A. Morton, D. Müller, A.R. Sahasransu, S. Tavernier, W. Van Doninck, P. Van Mulders

Université Libre de Bruxelles, Bruxelles, Belgium

D. Beghin, B. Bilin, B. Clerboux, G. De Lentdecker, L. Favart, A. Grebenyuk, A.K. Kalsi, K. Lee, M. Mahdavihorrani, I. Makarenko, L. Moureaux, L. Pétré, A. Popov, N. Postiau, E. Starling, L. Thomas, M. Vanden Bemden, C. Vander Velde, P. Vanlaer, D. Vannerom, L. Wezenbeek

Ghent University, Ghent, Belgium

T. Cornelis, D. Dobur, J. Knolle, L. Lambrecht, G. Mestdach, M. Niedziela, C. Roskas, A. Samalan, K. Skovpen, M. Tytgat, W. Verbeke, B. Vermassen, M. Vit

Université Catholique de Louvain, Louvain-la-Neuve, Belgium

A. Bethani, G. Bruno, F. Bury, C. Caputo, P. David, C. Delaere, I.S. Donertas, A. Giammanco, K. Jaffel, Sa. Jain, V. Lemaître, K. Mondal, J. Prisciandaro, A. Taliercio, M. Teklishyn, T.T. Tran, P. Vischia, S. Wertz

Centro Brasileiro de Pesquisas Físicas, Rio de Janeiro, Brazil

G.A. Alves, C. Hensel, A. Moraes

Universidade do Estado do Rio de Janeiro, Rio de Janeiro, Brazil

W.L. Aldá Júnior, M. Alves Gallo Pereira, M. Barroso Ferreira Filho, H. BRANDAO MALBOUISSON, W. Carvalho, J. Chinellato⁴, E.M. Da Costa, G.G. Da Silveira⁵, D. De Jesus Damiao, S. Fonseca De Souza, D. Matos Figueiredo, C. Mora Herrera, K. Mota Amarilo, L. Mundim, H. Nogima, P. Rebello Teles, A. Santoro, S.M. Silva Do Amaral, A. Sznajder, M. Thiel, F. Torres Da Silva De Araujo, A. Vilela Pereira

Universidade Estadual Paulista ^a, Universidade Federal do ABC ^b, São Paulo, Brazil

C.A. Bernardes^{a,a,5}, L. Calligaris^a, T.R. Fernandez Perez Tomei^a, E.M. Gregores^{a,b}, D.S. Lemos^a, P.G. Mercadante^{a,b}, S.F. Novaes^a, Sandra S. Padula^a

Institute for Nuclear Research and Nuclear Energy, Bulgarian Academy of Sciences, Sofia, Bulgaria

A. Aleksandrov, G. Antchev, R. Hadjiiska, P. Iaydjiev, M. Misheva, M. Rodozov, M. Shopova, G. Sultanov

University of Sofia, Sofia, Bulgaria

A. Dimitrov, T. Ivanov, L. Litov, B. Pavlov, P. Petkov, A. Petrov

Beihang University, Beijing, China

T. Cheng, Q. Guo, T. Javaid⁶, M. Mittal, H. Wang, L. Yuan

Department of Physics, Tsinghua University, Beijing, China

M. Ahmad, G. Bauer, C. Dozen⁷, Z. Hu, J. Martins⁸, Y. Wang, K. Yi^{9,10}

Institute of High Energy Physics, Beijing, China

E. Chapon, G.M. Chen⁶, H.S. Chen⁶, M. Chen, F. Iemmi, A. Kapoor, D. Leggat, H. Liao, Z.-A. LIU⁶, V. Milosevic, F. Monti, R. Sharma, J. Tao, J. Thomas-wilsker, J. Wang, H. Zhang, S. Zhang⁶, J. Zhao

State Key Laboratory of Nuclear Physics and Technology, Peking University, Beijing, China

A. Agapitos, Y. Ban, C. Chen, Q. Huang, A. Levin, Q. Li, X. Lyu, Y. Mao, S.J. Qian, D. Wang, Q. Wang, J. Xiao

Sun Yat-Sen University, Guangzhou, China

M. Lu, Z. You

Institute of Modern Physics and Key Laboratory of Nuclear Physics and Ion-beam Application (MOE) - Fudan University, Shanghai, China

X. Gao³, H. Okawa

Zhejiang University, Hangzhou, China

Z. Lin, M. Xiao

Universidad de Los Andes, Bogota, Colombia

C. Avila, A. Cabrera, C. Florez, J. Fraga, A. Sarkar, M.A. Segura Delgado

Universidad de Antioquia, Medellin, Colombia

J. Mejia Guisao, F. Ramirez, J.D. Ruiz Alvarez, C.A. Salazar González

University of Split, Faculty of Electrical Engineering, Mechanical Engineering and Naval Architecture, Split, Croatia

D. Giljanovic, N. Godinovic, D. Lelas, I. Puljak

University of Split, Faculty of Science, Split, Croatia

Z. Antunovic, M. Kovac, T. Sculac

Institute Rudjer Boskovic, Zagreb, Croatia

V. Brigljevic, D. Ferencek, D. Majumder, M. Roguljic, A. Starodumov¹¹, T. Susa

University of Cyprus, Nicosia, Cyprus

A. Attikis, K. Christoforou, E. Erodotou, A. Ioannou, G. Kole, M. Kolosova, S. Konstantinou, J. Mousa, C. Nicolaou, F. Ptochos, P.A. Razis, H. Rykaczewski, H. Saka

Charles University, Prague, Czech Republic

M. Finger¹², M. Finger Jr.¹², A. Kveton

Escuela Politecnica Nacional, Quito, Ecuador

E. Ayala

Universidad San Francisco de Quito, Quito, Ecuador

E. Carrera Jarrin

Academy of Scientific Research and Technology of the Arab Republic of Egypt, Egyptian Network of High Energy Physics, Cairo, Egypt

A.A. Abdelalim^{13,14}, E. Salama^{15,16}

Center for High Energy Physics (CHEP-FU), Fayoum University, El-Fayoum, Egypt

M.A. Mahmoud, Y. Mohammed

National Institute of Chemical Physics and Biophysics, Tallinn, Estonia

S. Bhowmik, A. Carvalho Antunes De Oliveira, R.K. Dewanjee, K. Ehataht, M. Kadastik, S. Nandan, C. Nielsen, J. Pata, M. Raidal, L. Tani, C. Veelken

Department of Physics, University of Helsinki, Helsinki, Finland

P. Eerola, L. Forthomme, H. Kirschenmann, K. Osterberg, M. Voutilainen

Helsinki Institute of Physics, Helsinki, Finland

S. Bharthuar, E. Brücken, F. Garcia, J. Havukainen, M.S. Kim, R. Kinnunen, T. Lampén, K. Lassila-Perini, S. Lehti, T. Lindén, M. Lotti, L. Martikainen, M. Myllymäki, J. Ott, H. Siikonen, E. Tuominen, J. Tuominiemi

Lappeenranta University of Technology, Lappeenranta, Finland

P. Luukka, H. Petrow, T. Tuuva

IRFU, CEA, Université Paris-Saclay, Gif-sur-Yvette, France

C. Amendola, M. Besancon, F. Couderc, M. Dejardin, D. Denegri, J.L. Faure, F. Ferri, S. Ganjour, A. Givernaud, P. Gras, G. Hamel de Monchenault, P. Jarry, B. Lenzi, E. Locci, J. Malcles, J. Rander, A. Rosowsky, M.Ö. Sahin, A. Savoy-Navarro¹⁷, M. Titov, G.B. Yu

Laboratoire Leprince-Ringuet, CNRS/IN2P3, Ecole Polytechnique, Institut Polytechnique de Paris, Palaiseau, France

S. Ahuja, F. Beaudette, M. Bonanomi, A. Buchot Perraguin, P. Busson, A. Cappati, C. Charlot, O. Davignon, B. Diab, G. Falmagne, S. Ghosh, R. Granier de Cassagnac, A. Hakimi, I. Kucher, M. Nguyen, C. Ochando, P. Paganini, J. Rembser, R. Salerno, J.B. Sauvan, Y. Sirois, A. Zabi, A. Zghiche

Université de Strasbourg, CNRS, IPHC UMR 7178, Strasbourg, France

J.-L. Agram¹⁸, J. Andrea, D. Apparau, D. Bloch, G. Bourgatte, J.-M. Brom, E.C. Chabert, C. Collard, D. Darej, J.-C. Fontaine¹⁸, U. Goerlach, C. Grimault, A.-C. Le Bihan, E. Nibigira, P. Van Hove

Institut de Physique des 2 Infinis de Lyon (IP2I), Villeurbanne, France

E. Asilar, S. Beauceron, C. Bernet, G. Boudoul, C. Camen, A. Carle, N. Chanon, D. Contardo, P. Depasse, H. El Mamouni, J. Fay, S. Gascon, M. Gouzevitch, B. Ille, I.B. Laktineh, H. Lattaud, A. Lesauvage, M. Lethuillier, L. Mirabito, S. Perries, K. Shchablo, V. Sordini, L. Torterotot, G. Touquet, M. Vander Donckt, S. Viret

Georgian Technical University, Tbilisi, Georgia

A. Khvedelidze¹², I. Lomidze, Z. Tsamalaidze¹²

RWTH Aachen University, I. Physikalisches Institut, Aachen, Germany

L. Feld, K. Klein, M. Lipinski, D. Meuser, A. Pauls, M.P. Rauch, N. Röwert, J. Schulz, M. Teroerde

RWTH Aachen University, III. Physikalisches Institut A, Aachen, Germany

A. Dodonova, D. Eliseev, M. Erdmann, P. Fackeldey, B. Fischer, S. Ghosh, T. Hebbeker, K. Hoepfner, F. Ivone, H. Keller, L. Mastrolorenzo, M. Merschmeyer, A. Meyer, G. Mocellin,

S. Mondal, S. Mukherjee, D. Noll, A. Novak, T. Pook, A. Pozdnyakov, Y. Rath, H. Reithler, J. Roemer, A. Schmidt, S.C. Schuler, A. Sharma, L. Vigilante, S. Wiedenbeck, S. Zaleski

RWTH Aachen University, III. Physikalisches Institut B, Aachen, Germany

C. Dziwok, G. Flügge, W. Haj Ahmad¹⁹, O. Hlushchenko, T. Kress, A. Nowack, C. Pistone, O. Pooth, D. Roy, H. Sert, A. Stahl²⁰, T. Ziemons

Deutsches Elektronen-Synchrotron, Hamburg, Germany

H. Aarup Petersen, M. Aldaya Martin, P. Asmuss, I. Babounikau, S. Baxter, O. Behnke, A. Bermúdez Martínez, S. Bhattacharya, A.A. Bin Anuar, K. Borras²¹, V. Botta, D. Brunner, A. Campbell, A. Cardini, C. Cheng, F. Colombina, S. Consuegra Rodríguez, G. Correia Silva, V. Danilov, L. Didukh, G. Eckerlin, D. Eckstein, L.I. Estevez Banos, O. Filatov, E. Gallo²², A. Geiser, A. Giraldi, A. Grohsjean, M. Guthoff, A. Jafari²³, N.Z. Jomhari, H. Jung, A. Kasem²¹, M. Kasemann, H. Kaveh, C. Kleinwort, D. Krücker, W. Lange, J. Lidrych, K. Lipka, W. Lohmann²⁴, R. Mankel, I.-A. Melzer-Pellmann, J. Metwally, A.B. Meyer, M. Meyer, J. Mnich, A. Mussgiller, Y. Otariid, D. Pérez Adán, D. Pitzl, A. Raspereza, B. Ribeiro Lopes, J. Rübenach, A. Saggio, A. Saibel, M. Savitskyi, M. Scham, V. Scheurer, C. Schwanenberger²², A. Singh, R.E. Sosa Ricardo, D. Stafford, N. Tonon, O. Turkot, M. Van De Klundert, R. Walsh, D. Walter, Y. Wen, K. Wichmann, L. Wiens, C. Wissing, S. Wuchterl

University of Hamburg, Hamburg, Germany

R. Aggleton, S. Albrecht, S. Bein, L. Benato, A. Benecke, P. Connor, K. De Leo, M. Eich, F. Feindt, A. Fröhlich, C. Garbers, E. Garutti, P. Gunnellini, J. Haller, A. Hinzmann, G. Kasieczka, R. Klanner, R. Kogler, T. Kramer, V. Kutzner, J. Lange, T. Lange, A. Lobanov, A. Malara, A. Nigamova, K.J. Pena Rodriguez, O. Rieger, P. Schleper, M. Schröder, J. Schwandt, D. Schwarz, J. Sonneveld, H. Stadie, G. Steinbrück, A. Tews, B. Vormwald, I. Zoi

Karlsruher Institut fuer Technologie, Karlsruhe, Germany

J. Bechtel, T. Berger, E. Butz, R. Caspart, T. Chwalek, W. De Boer[†], A. Dierlamm, A. Droll, K. El Morabit, N. Faltermann, M. Giffels, J.o. Gosewisch, A. Gottmann, F. Hartmann²⁰, C. Heidecker, U. Husemann, I. Katkov²⁵, P. Keicher, R. Koppenhöfer, S. Maier, M. Metzler, S. Mitra, Th. Müller, M. Neukum, A. Nürnberg, G. Quast, K. Rabbertz, J. Rauser, D. Savoie, M. Schnepf, D. Seith, I. Shvetsov, H.J. Simonis, R. Ulrich, J. Van Der Linden, R.F. Von Cube, M. Wassmer, M. Weber, S. Wieland, R. Wolf, S. Wozniewski, S. Wunsch

Institute of Nuclear and Particle Physics (INPP), NCSR Demokritos, Aghia Paraskevi, Greece

G. Anagnostou, G. Daskalakis, T. Gerasis, A. Kyriakis, D. Loukas, A. Stakia

National and Kapodistrian University of Athens, Athens, Greece

M. Diamantopoulou, D. Karasavvas, G. Karathanasis, P. Kontaxakis, C.K. Koraka, A. Manousakis-katsikakis, A. Panagiotou, I. Papavergou, N. Saoulidou, K. Theofilatos, E. Tziaferi, K. Vellidis, E. Vourliotis

National Technical University of Athens, Athens, Greece

G. Bakas, K. Kousouris, I. Papakrivopoulos, G. Tsipolitis, A. Zacharopoulou

University of Ioánnina, Ioánnina, Greece

I. Evangelou, C. Foudas, P. Giannelos, P. Katsoulis, P. Kokkas, N. Manthos, I. Papadopoulos, J. Strologas

MTA-ELTE Lendület CMS Particle and Nuclear Physics Group, Eötvös Loránd University,

Budapest, Hungary

M. Csanad, K. Farkas, M.M.A. Gadallah²⁶, S. Lökös²⁷, P. Major, K. Mandal, A. Mehta, G. Pasztor, A.J. Rádl, O. Surányi, G.I. Veres

Wigner Research Centre for Physics, Budapest, Hungary

M. Bartók²⁸, G. Bencze, C. Hajdu, D. Horvath²⁹, F. Sikler, V. Veszpremi, G. Vesztergombi[†]

Institute of Nuclear Research ATOMKI, Debrecen, Hungary

S. Czellar, J. Karancsi²⁸, J. Molnar, Z. Szillasi, D. Teyssier

Institute of Physics, University of Debrecen, Debrecen, Hungary

P. Raics, Z.L. Trocsanyi³⁰, B. Ujvari

Karoly Robert Campus, MATE Institute of Technology

T. Csorgo³¹, F. Nemes³¹, T. Novak

Indian Institute of Science (IISc), Bangalore, India

J.R. Komaragiri, D. Kumar, L. Panwar, P.C. Tiwari

National Institute of Science Education and Research, HBNI, Bhubaneswar, India

S. Bahinipati³², C. Kar, P. Mal, T. Mishra, V.K. Muraleedharan Nair Bindhu³³, A. Nayak³³, P. Saha, N. Sur, S.K. Swain, D. Vats³³

Panjab University, Chandigarh, India

S. Bansal, S.B. Beri, V. Bhatnagar, G. Chaudhary, S. Chauhan, N. Dhingra³⁴, R. Gupta, A. Kaur, M. Kaur, S. Kaur, P. Kumari, M. Meena, K. Sandeep, J.B. Singh, A.K. Viridi

University of Delhi, Delhi, India

A. Ahmed, A. Bhardwaj, B.C. Choudhary, M. Gola, S. Keshri, A. Kumar, M. Naimuddin, P. Priyanka, K. Ranjan, A. Shah

Saha Institute of Nuclear Physics, HBNI, Kolkata, India

M. Bharti³⁵, R. Bhattacharya, S. Bhattacharya, D. Bhowmik, S. Dutta, S. Dutta, B. Gomber³⁶, M. Maity³⁷, P. Palit, P.K. Rout, G. Saha, B. Sahu, S. Sarkar, M. Sharan, B. Singh³⁵, S. Thakur³⁵

Indian Institute of Technology Madras, Madras, India

P.K. Behera, S.C. Behera, P. Kalbhor, A. Muhammad, R. Pradhan, P.R. Pujahari, A. Sharma, A.K. Sikdar

Bhabha Atomic Research Centre, Mumbai, India

D. Dutta, V. Jha, V. Kumar, D.K. Mishra, K. Naskar³⁸, P.K. Netrakanti, L.M. Pant, P. Shukla

Tata Institute of Fundamental Research-A, Mumbai, India

T. Aziz, S. Dugad, M. Kumar, U. Sarkar

Tata Institute of Fundamental Research-B, Mumbai, India

S. Banerjee, R. Chudasama, M. Guchait, S. Karmakar, S. Kumar, G. Majumder, K. Mazumdar, S. Mukherjee

Indian Institute of Science Education and Research (IISER), Pune, India

K. Alpana, S. Dube, B. Kansal, A. Laha, S. Pandey, A. Rane, A. Rastogi, S. Sharma

Department of Physics, Isfahan University of Technology, Isfahan, Iran

H. Bakhshiansohi³⁹, M. Zeinali⁴⁰

Institute for Research in Fundamental Sciences (IPM), Tehran, Iran

S. Chenarani⁴¹, S.M. Etesami, M. Khakzad, M. Mohammadi Najafabadi

University College Dublin, Dublin, Ireland

M. Grunewald

INFN Sezione di Bari ^a, Università di Bari ^b, Politecnico di Bari ^c, Bari, Italy

M. Abbrescia^{a,b}, R. Aly^{a,b,42}, C. Aruta^{a,b}, A. Colaleo^a, D. Creanza^{a,c}, N. De Filippis^{a,c}, M. De Palma^{a,b}, A. Di Florio^{a,b}, A. Di Pilato^{a,b}, W. Elmetenawee^{a,b}, L. Fiore^a, A. Gelmi^{a,b}, M. Gul^a, G. Iaselli^{a,c}, M. Ince^{a,b}, S. Lezki^{a,b}, G. Maggi^{a,c}, M. Maggi^a, I. Margjeka^{a,b}, V. Mastrapasqua^{a,b}, J.A. Merlin^a, S. My^{a,b}, S. Nuzzo^{a,b}, A. Pellecchia^{a,b}, A. Pompili^{a,b}, G. Pugliese^{a,c}, A. Ranieri^a, G. Selvaggi^{a,b}, L. Silvestris^a, F.M. Simone^{a,b}, R. Venditti^a, P. Verwilligen^a

INFN Sezione di Bologna ^a, Università di Bologna ^b, Bologna, Italy

G. Abbiendi^a, C. Battilana^{a,b}, D. Bonacorsi^{a,b}, L. Borgonovi^a, L. Brigliadori^a, R. Campanini^{a,b}, P. Capiluppi^{a,b}, A. Castro^{a,b}, F.R. Cavallo^a, M. Cuffiani^{a,b}, G.M. Dallavalle^a, T. Diotallevi^{a,b}, F. Fabbrì^a, A. Fanfani^{a,b}, P. Giacomelli^a, L. Giommi^{a,b}, C. Grandi^a, L. Guiducci^{a,b}, S. Lo Meo^{a,43}, L. Lunerti^{a,b}, S. Marcellini^a, G. Masetti^a, F.L. Navarra^{a,b}, A. Perrotta^a, F. Primavera^{a,b}, A.M. Rossi^{a,b}, T. Rovelli^{a,b}, G.P. Siroli^{a,b}

INFN Sezione di Catania ^a, Università di Catania ^b, Catania, Italy

S. Albergo^{a,b,44}, S. Costa^{a,b,44}, A. Di Mattia^a, R. Potenza^{a,b}, A. Tricomi^{a,b,44}, C. Tuve^{a,b}

INFN Sezione di Firenze ^a, Università di Firenze ^b, Firenze, Italy

G. Barbagli^a, A. Cassese^a, R. Ceccarelli^{a,b}, V. Ciulli^{a,b}, C. Civinini^a, R. D'Alessandro^{a,b}, E. Focardi^{a,b}, G. Latino^{a,b}, P. Lenzi^{a,b}, M. Lizzo^{a,b}, M. Meschini^a, S. Paoletti^a, R. Seidita^{a,b}, G. Sguazzoni^a, L. Viliani^a

INFN Laboratori Nazionali di Frascati, Frascati, Italy

L. Benussi, S. Bianco, D. Piccolo

INFN Sezione di Genova ^a, Università di Genova ^b, Genova, Italy

M. Bozzo^{a,b}, F. Ferro^a, R. Mulargia^{a,b}, E. Robutti^a, S. Tosi^{a,b}

INFN Sezione di Milano-Bicocca ^a, Università di Milano-Bicocca ^b, Milano, Italy

A. Benaglia^a, F. Brivio^{a,b}, F. Cetorelli^{a,b}, V. Ciriolo^{a,b,20}, F. De Guio^{a,b}, M.E. Dinardo^{a,b}, P. Dini^a, S. Gennai^a, A. Ghezzi^{a,b}, P. Govoni^{a,b}, L. Guzzi^{a,b}, M. Malberti^a, S. Malvezzi^a, A. Massironi^a, D. Menasce^a, L. Moroni^a, M. Paganoni^{a,b}, D. Pedrini^a, S. Ragazzi^{a,b}, N. Redaelli^a, T. Tabarelli de Fatis^{a,b}, D. Valsecchi^{a,b,20}, D. Zuolo^{a,b}

INFN Sezione di Napoli ^a, Università di Napoli 'Federico II' ^b, Napoli, Italy, Università della Basilicata ^c, Potenza, Italy, Università G. Marconi ^d, Roma, Italy

S. Buontempo^a, F. Carnevali^{a,b}, N. Cavallo^{a,c}, A. De Iorio^{a,b}, F. Fabozzi^{a,c}, A.O.M. Iorio^{a,b}, L. Lista^{a,b}, S. Meola^{a,d,20}, P. Paolucci^{a,20}, B. Rossi^a, C. Sciacca^{a,b}

INFN Sezione di Padova ^a, Università di Padova ^b, Padova, Italy, Università di Trento ^c, Trento, Italy

P. Azzi^a, N. Bacchetta^a, D. Bisello^{a,b}, P. Bortignon^a, A. Bragagnolo^{a,b}, R. Carlin^{a,b}, P. Checchia^a, T. Dorigo^a, U. Dosselli^a, F. Gasparini^{a,b}, U. Gasparini^{a,b}, S.Y. Hoh^{a,b}, L. Layer^{a,45}, M. Margoni^{a,b}, A.T. Meneguzzo^{a,b}, J. Pazzini^{a,b}, M. Presilla^{a,b}, P. Ronchese^{a,b}, R. Rossin^{a,b}, F. Simonetto^{a,b}, G. Strong^a, M. Tosi^{a,b}, H. YARAR^{a,b}, M. Zanetti^{a,b}, P. Zotto^{a,b}, A. Zucchetta^{a,b}, G. Zumerle^{a,b}

INFN Sezione di Pavia ^a, Università di Pavia ^b, Pavia, Italy

C. Aime^{a,b}, A. Braghieri^a, S. Calzaferri^{a,b}, D. Fiorina^{a,b}, P. Montagna^{a,b}, S.P. Ratti^{a,b}, V. Re^a, C. Riccardi^{a,b}, P. Salvini^a, I. Vai^a, P. Vitulo^{a,b}

INFN Sezione di Perugia ^a, Università di Perugia ^b, Perugia, Italy

P. Asenov^{a,46}, G.M. Bilei^a, D. Ciangottini^{a,b}, L. Fanò^{a,b}, P. Lariccia^{a,b}, M. Magherini^b, G. Mantovani^{a,b}, V. Mariani^{a,b}, M. Menichelli^a, F. Moscatelli^{a,46}, A. Piccinelli^{a,b}, A. Rossi^{a,b}, A. Santocchia^{a,b}, D. Spiga^a, T. Tedeschi^{a,b}

INFN Sezione di Pisa ^a, Università di Pisa ^b, Scuola Normale Superiore di Pisa ^c, Pisa Italy, Università di Siena ^d, Siena, Italy

P. Azzurri^a, G. Bagliesi^a, V. Bertacchi^{a,c}, L. Bianchini^a, T. Boccali^a, E. Bossini^{a,b}, R. Castaldi^a, M.A. Ciocci^{a,b}, V. D'Amante^{a,d}, R. Dell'Orso^a, M.R. Di Domenico^{a,d}, S. Donato^a, A. Giassi^a, F. Ligabue^{a,c}, E. Manca^{a,c}, G. Mandorli^{a,c}, A. Messineo^{a,b}, F. Palla^a, S. Parolia^{a,b}, G. Ramirez-Sanchez^{a,c}, A. Rizzi^{a,b}, G. Rolandi^{a,c}, S. Roy Chowdhury^{a,c}, A. Scribano^a, N. Shafiei^{a,b}, P. Spagnolo^a, R. Tenchini^a, G. Tonelli^{a,b}, N. Turini^{a,d}, A. Venturi^a, P.G. Verdini^a

INFN Sezione di Roma ^a, Sapienza Università di Roma ^b, Rome, Italy

M. Campana^{a,b}, F. Cavallari^a, M. Cipriani^{a,b}, D. Del Re^{a,b}, E. Di Marco^a, M. Diemoz^a, E. Longo^{a,b}, P. Meridiani^a, G. Organtini^{a,b}, F. Pandolfi^a, R. Paramatti^{a,b}, C. Quaranta^{a,b}, S. Rahatlou^{a,b}, C. Rovelli^a, F. Santanastasio^{a,b}, L. Soffi^a, R. Tramontano^{a,b}

INFN Sezione di Torino ^a, Università di Torino ^b, Torino, Italy, Università del Piemonte Orientale ^c, Novara, Italy

N. Amapane^{a,b}, R. Arcidiacono^{a,c}, S. Argiro^{a,b}, M. Arneodo^{a,c}, N. Bartosik^a, R. Bellan^{a,b}, A. Bellora^{a,b}, J. Berenguer Antequera^{a,b}, C. Biino^a, N. Cartiglia^a, S. Cometti^a, M. Costa^{a,b}, R. Covarelli^{a,b}, N. Demaria^a, B. Kiani^{a,b}, F. Legger^a, C. Mariotti^a, S. Maselli^a, E. Migliore^{a,b}, E. Monteil^{a,b}, M. Monteno^a, M.M. Obertino^{a,b}, G. Ortona^a, L. Pacher^{a,b}, N. Pastrone^a, M. Pelliccioni^a, G.L. Pinna Angioni^{a,b}, M. Ruspa^{a,c}, K. Shchelina^{a,b}, F. Siviero^{a,b}, V. Sola^a, A. Solano^{a,b}, D. Soldi^{a,b}, A. Staiano^a, M. Tornago^{a,b}, D. Trocino^{a,b}, A. Vagnerini

INFN Sezione di Trieste ^a, Università di Trieste ^b, Trieste, Italy

S. Belforte^a, V. Candelise^{a,b}, M. Casarsa^a, F. Cossutti^a, A. Da Rold^{a,b}, G. Della Ricca^{a,b}, G. Sorrentino^{a,b}, F. Vazzoler^{a,b}

Kyungpook National University, Daegu, Korea

S. Dogra, C. Huh, B. Kim, D.H. Kim, G.N. Kim, J. Kim, J. Lee, S.W. Lee, C.S. Moon, Y.D. Oh, S.I. Pak, B.C. Radburn-Smith, S. Sekmen, Y.C. Yang

Chonnam National University, Institute for Universe and Elementary Particles, Kwangju, Korea

H. Kim, D.H. Moon

Hanyang University, Seoul, Korea

B. Francois, T.J. Kim, J. Park

Korea University, Seoul, Korea

S. Cho, S. Choi, Y. Go, B. Hong, K. Lee, K.S. Lee, J. Lim, J. Park, S.K. Park, J. Yoo

Kyung Hee University, Department of Physics, Seoul, Republic of Korea

J. Goh, A. Gurtu

Sejong University, Seoul, Korea

H.S. Kim, Y. Kim

Seoul National University, Seoul, Korea

J. Almond, J.H. Bhyun, J. Choi, S. Jeon, J. Kim, J.S. Kim, S. Ko, H. Kwon, H. Lee, S. Lee, B.H. Oh, M. Oh, S.B. Oh, H. Seo, U.K. Yang, I. Yoon

University of Seoul, Seoul, Korea

W. Jang, D. Jeon, D.Y. Kang, Y. Kang, J.H. Kim, S. Kim, B. Ko, J.S.H. Lee, Y. Lee, I.C. Park, Y. Roh, M.S. Ryu, D. Song, I.J. Watson, S. Yang

Yonsei University, Department of Physics, Seoul, Korea

S. Ha, H.D. Yoo

Sungkyunkwan University, Suwon, Korea

M. Choi, Y. Jeong, H. Lee, Y. Lee, I. Yu

College of Engineering and Technology, American University of the Middle East (AUM), Egaila, Kuwait

T. Beyrouthy, Y. Maghrbi

Riga Technical University, Riga, Latvia

T. Torims, V. Veckalns⁴⁷

Vilnius University, Vilnius, Lithuania

M. Ambrozys, A. Juodagalvis, A. Rinkevicius, G. Tamulaitis

National Centre for Particle Physics, Universiti Malaya, Kuala Lumpur, Malaysia

N. Bin Norjoharuddeen, W.A.T. Wan Abdullah, M.N. Yusli, Z. Zolkapli

Universidad de Sonora (UNISON), Hermosillo, Mexico

J.F. Benitez, A. Castaneda Hernandez, M. León Coello, J.A. Murillo Quijada, A. Sehwawat, L. Valencia Palomo

Centro de Investigacion y de Estudios Avanzados del IPN, Mexico City, Mexico

G. Ayala, H. Castilla-Valdez, E. De La Cruz-Burelo, I. Heredia-De La Cruz⁴⁸, R. Lopez-Fernandez, C.A. Mondragon Herrera, D.A. Perez Navarro, A. Sanchez-Hernandez

Universidad Iberoamericana, Mexico City, Mexico

S. Carrillo Moreno, C. Oropeza Barrera, M. Ramirez-Garcia, F. Vazquez Valencia

Benemerita Universidad Autonoma de Puebla, Puebla, Mexico

I. Pedraza, H.A. Salazar Ibarguen, C. Uribe Estrada

University of Montenegro, Podgorica, Montenegro

J. Mijuskovic⁴⁹, N. Raicevic

University of Auckland, Auckland, New Zealand

D. Krofcheck

University of Canterbury, Christchurch, New Zealand

S. Bheesette, P.H. Butler

National Centre for Physics, Quaid-I-Azam University, Islamabad, Pakistan

A. Ahmad, M.I. Asghar, A. Awais, M.I.M. Awan, H.R. Hoorani, W.A. Khan, M.A. Shah, M. Shoaib, M. Waqas

AGH University of Science and Technology Faculty of Computer Science, Electronics and Telecommunications, Krakow, Poland

V. Avati, L. Grzanka, M. Malawski

National Centre for Nuclear Research, Swierk, Poland

H. Bialkowska, M. Bluj, B. Boimska, M. Górski, M. Kazana, M. Szleper, P. Zalewski

Institute of Experimental Physics, Faculty of Physics, University of Warsaw, Warsaw, Poland
K. Bunkowski, K. Doroba, A. Kalinowski, M. Konecki, J. Krolikowski, M. Walczak

Laboratório de Instrumentação e Física Experimental de Partículas, Lisboa, Portugal
M. Araujo, P. Bargassa, D. Bastos, A. Boletti, P. Faccioli, M. Gallinaro, J. Hollar, N. Leonardo, T. Niknejad, M. Pisano, J. Seixas, O. Toldaiev, J. Varela

Joint Institute for Nuclear Research, Dubna, Russia
S. Afanasiev, D. Budkouski, I. Golutvin, I. Gorbunov, V. Karjavine, V. Korenkov, A. Lanev, A. Malakhov, V. Matveev^{50,51}, V. Palichik, V. Perelygin, M. Savina, D. Seitova, V. Shalaev, S. Shmatov, S. Shulha, V. Smirnov, O. Teryaev, N. Voytishin, B.S. Yuldashev⁵², A. Zarubin, I. Zhizhin

Petersburg Nuclear Physics Institute, Gatchina (St. Petersburg), Russia
G. Gavrillov, V. Golovtsov, Y. Ivanov, V. Kim⁵³, E. Kuznetsova⁵⁴, V. Murzin, V. Oreshkin, I. Smirnov, D. Sosnov, V. Sulimov, L. Uvarov, S. Volkov, A. Vorobyev

Institute for Nuclear Research, Moscow, Russia
Yu. Andreev, A. Dermenev, S. Gninenko, N. Golubev, A. Karneyeu, D. Kirpichnikov, M. Kirsanov, N. Krasnikov, A. Pashenkov, G. Pivovarov, D. Tlisov[†], A. Toropin

Institute for Theoretical and Experimental Physics named by A.I. Alikhanov of NRC 'Kurchatov Institute', Moscow, Russia
V. Epshteyn, V. Gavrillov, N. Lychkovskaya, A. Nikitenko⁵⁵, V. Popov, A. Spiridonov, A. Stepenov, M. Toms, E. Vlasov, A. Zhokin

Moscow Institute of Physics and Technology, Moscow, Russia
T. Aushev

National Research Nuclear University 'Moscow Engineering Physics Institute' (MEPhI), Moscow, Russia
M. Chadeeva⁵⁶, A. Oskin, P. Parygin, E. Popova, V. Rusinov

P.N. Lebedev Physical Institute, Moscow, Russia
V. Andreev, M. Azarkin, I. Dremin, M. Kirakosyan, A. Terkulov

Skobeltsyn Institute of Nuclear Physics, Lomonosov Moscow State University, Moscow, Russia
A. Belyaev, E. Boos, M. Dubinin⁵⁷, L. Dudko, A. Ershov, A. Gribushin, V. Klyukhin, O. Kodolova, I. Lokhtin, S. Obraztsov, S. Petrushanko, V. Savrin, A. Snigirev

Novosibirsk State University (NSU), Novosibirsk, Russia
V. Blinov⁵⁸, T. Dimova⁵⁸, L. Kardapoltsev⁵⁸, A. Kozyrev⁵⁸, I. Ovtin⁵⁸, Y. Skovpen⁵⁸

Institute for High Energy Physics of National Research Centre 'Kurchatov Institute', Protvino, Russia
I. Azhgirey, I. Bayshev, D. Elumakhov, V. Kachanov, D. Konstantinov, P. Mandrik, V. Petrov, R. Ryutin, S. Slabospitskii, A. Sobol, S. Troshin, N. Tyurin, A. Uzunian, A. Volkov

National Research Tomsk Polytechnic University, Tomsk, Russia
A. Babaev, V. Okhotnikov

Tomsk State University, Tomsk, Russia
V. Borshch, V. Ivanchenko, E. Tcherniaev

University of Belgrade: Faculty of Physics and VINCA Institute of Nuclear Sciences, Belgrade, Serbia

P. Adzic⁵⁹, M. Dordevic, P. Milenovic, J. Milosevic

Centro de Investigaciones Energéticas Medioambientales y Tecnológicas (CIEMAT), Madrid, Spain

M. Aguilar-Benitez, J. Alcaraz Maestre, A. Álvarez Fernández, I. Bachiller, M. Barrio Luna, Cristina F. Bedoya, C.A. Carrillo Montoya, M. Cepeda, M. Cerrada, N. Colino, B. De La Cruz, A. Delgado Peris, J.P. Fernández Ramos, J. Flix, M.C. Fouz, O. Gonzalez Lopez, S. Goy Lopez, J.M. Hernandez, M.I. Josa, J. León Holgado, D. Moran, Á. Navarro Tobar, A. Pérez-Calero Yzquierdo, J. Puerta Pelayo, I. Redondo, L. Romero, S. Sánchez Navas, L. Urda Gómez, C. Willmott

Universidad Autónoma de Madrid, Madrid, Spain

J.F. de Trocóniz, R. Reyes-Almanza

Universidad de Oviedo, Instituto Universitario de Ciencias y Tecnologías Espaciales de Asturias (ICTEA), Oviedo, Spain

B. Alvarez Gonzalez, J. Cuevas, C. Erice, J. Fernandez Menendez, S. Folgueras, I. Gonzalez Caballero, J.R. González Fernández, E. Palencia Cortezon, C. Ramón Álvarez, J. Ripoll Sau, V. Rodríguez Bouza, A. Trapote, N. Trevisani

Instituto de Física de Cantabria (IFCA), CSIC-Universidad de Cantabria, Santander, Spain

J.A. Brochero Cifuentes, I.J. Cabrillo, A. Calderon, J. Duarte Campderros, M. Fernandez, C. Fernandez Madrazo, P.J. Fernández Manteca, A. García Alonso, G. Gomez, C. Martinez Rivero, P. Martinez Ruiz del Arbol, F. Matorras, P. Matorras Cuevas, J. Piedra Gomez, C. Prieels, T. Rodrigo, A. Ruiz-Jimeno, L. Scodellaro, I. Vila, J.M. Vizan Garcia

University of Colombo, Colombo, Sri Lanka

MK Jayananda, B. Kailasapathy⁶⁰, D.U.J. Sonnadara, DDC Wickramarathna

University of Ruhuna, Department of Physics, Matara, Sri Lanka

W.G.D. Dharmaratna, K. Liyanage, N. Perera, N. Wickramage

CERN, European Organization for Nuclear Research, Geneva, Switzerland

T.K. Aarrestad, D. Abbaneo, J. Alimena, E. Auffray, G. Auzinger, J. Baechler, P. Baillon[†], D. Barney, J. Bendavid, M. Bianco, A. Bocci, T. Camporesi, M. Capeans Garrido, G. Cerminara, S.S. Chhibra, L. Cristella, D. d'Enterria, A. Dabrowski, N. Daci, A. David, A. De Roeck, M.M. Defranchis, M. Deile, M. Dobson, M. Dünser, N. Dupont, A. Elliott-Peisert, N. Emriskova, F. Fallavollita⁶¹, D. Fasanella, S. Fiorendi, A. Florent, G. Franzoni, W. Funk, S. Giani, D. Gigi, K. Gill, F. Glege, L. Gouskos, M. Haranko, J. Hegeman, Y. Iiyama, V. Innocente, T. James, P. Janot, J. Kaspar, J. Kieseler, M. Komm, N. Kratochwil, C. Lange, S. Laurila, P. Lecoq, K. Long, C. Lourenço, L. Malgeri, S. Mallios, M. Mannelli, A.C. Marini, F. Meijers, S. Mersi, E. Meschi, F. Moortgat, M. Mulders, S. Orfanelli, L. Orsini, F. Pantaleo, L. Pape, E. Perez, M. Peruzzi, A. Petrilli, G. Petrucciani, A. Pfeiffer, M. Pierini, D. Piparo, M. Pitt, H. Qu, T. Quast, D. Rabady, A. Racz, G. Reales Gutiérrez, M. Rieger, M. Rovere, H. Sakulin, J. Salfeld-Nebgen, S. Scarfi, C. Schäfer, C. Schwick, M. Selvaggi, A. Sharma, P. Silva, W. Snoeys, P. Sphicas⁶², S. Summers, V.R. Tavolaro, D. Treille, A. Tsiros, G.P. Van Onsem, M. Verzetti, J. Wanczyk⁶³, K.A. Wozniak, W.D. Zeuner

Paul Scherrer Institut, Villigen, Switzerland

L. Caminada⁶⁴, A. Ebrahimi, W. Erdmann, R. Horisberger, Q. Ingram, H.C. Kaestli, D. Kotlinski, U. Langenegger, M. Missiroli, T. Rohe

ETH Zurich - Institute for Particle Physics and Astrophysics (IPA), Zurich, Switzerland

K. Androsov⁶³, M. Backhaus, P. Berger, A. Calandri, N. Chernyavskaya, A. De Cosa, G. Dissertori, M. Dittmar, M. Donegà, C. Dorfer, F. Eble, K. Gedia, F. Glessgen, T.A. Gómez Espinosa, C. Grab, D. Hits, W. Lusterhmann, A.-M. Lyon, R.A. Manzoni, C. Martin Perez, M.T. Meinhard, F. Nessi-Tedaldi, J. Niedziela, F. Pauss, V. Perovic, S. Pigazzini, M.G. Ratti, M. Reichmann, C. Reissel, T. Reitenspiess, B. Ristic, D. Ruini, D.A. Sanz Becerra, M. Schönenberger, V. Stampf, J. Steggemann⁶³, R. Wallny, D.H. Zhu

Universität Zürich, Zurich, Switzerland

C. Amsler⁶⁵, P. Bäertschi, C. Botta, D. Brzhechko, M.F. Canelli, K. Cormier, A. De Wit, R. Del Burgo, J.K. Heikkilä, M. Huwiler, A. Jofrehei, B. Kilminster, S. Leontsinis, A. Macchiolo, P. Meiring, V.M. Mikuni, U. Molinatti, I. Neutelings, A. Reimers, P. Robmann, S. Sanchez Cruz, K. Schweiger, Y. Takahashi

National Central University, Chung-Li, Taiwan

C. Adloff⁶⁶, C.M. Kuo, W. Lin, A. Roy, T. Sarkar³⁷, S.S. Yu

National Taiwan University (NTU), Taipei, Taiwan

L. Ceard, Y. Chao, K.F. Chen, P.H. Chen, W.-S. Hou, Y.y. Li, R.-S. Lu, E. Paganis, A. Psallidas, A. Steen, H.y. Wu, E. Yazgan, P.r. Yu

Chulalongkorn University, Faculty of Science, Department of Physics, Bangkok, Thailand

B. Asavapibhop, C. Asawatangtrakuldee, N. Srimanobhas

Çukurova University, Physics Department, Science and Art Faculty, Adana, Turkey

F. Boran, S. Damarseckin⁶⁷, Z.S. Demiroglu, F. Dolek, I. Dumanoglu⁶⁸, E. Eskut, Y. Guler, E. Gurpinar Guler⁶⁹, I. Hos⁷⁰, C. Isik, O. Kara, A. Kayis Topaksu, U. Kiminsu, G. Onengut, K. Ozdemir⁷¹, A. Polatoz, A.E. Simsek, B. Tali⁷², U.G. Tok, S. Turkcapar, I.S. Zorbakir, C. Zorbilmez

Middle East Technical University, Physics Department, Ankara, Turkey

B. Isildak⁷³, G. Karapinar⁷⁴, K. Ocalan⁷⁵, M. Yalvac⁷⁶

Bogazici University, Istanbul, Turkey

B. Akgun, I.O. Atakisi, E. Gülmez, M. Kaya⁷⁷, O. Kaya⁷⁸, Ö. Özçelik, S. Tekten⁷⁹, E.A. Yetkin⁸⁰

Istanbul Technical University, Istanbul, Turkey

A. Cakir, K. Cankocak⁶⁸, Y. Komurcu, S. Sen⁸¹

Istanbul University, Istanbul, Turkey

S. Cerci⁷², B. Kaynak, S. Ozkorucuklu, D. Sunar Cerci⁷²

Institute for Scintillation Materials of National Academy of Science of Ukraine, Kharkov, Ukraine

B. Grynyov

National Scientific Center, Kharkov Institute of Physics and Technology, Kharkov, Ukraine

L. Levchuk

University of Bristol, Bristol, United Kingdom

D. Anthony, E. Bhal, S. Bologna, J.J. Brooke, A. Bundock, E. Clement, D. Cussans, H. Flacher, J. Goldstein, G.P. Heath, H.F. Heath, M.I. Holmberg⁸², L. Kreczko, B. Krikler, S. Paramesvaran, S. Seif El Nasr-Storey, V.J. Smith, N. Stylianou⁸³, K. Walkingshaw Pass, R. White

Rutherford Appleton Laboratory, Didcot, United Kingdom

K.W. Bell, A. Belyaev⁸⁴, C. Brew, R.M. Brown, D.J.A. Cockerill, C. Cooke, K.V. Ellis, K. Harder,

S. Harper, J. Linacre, K. Manolopoulos, D.M. Newbold, E. Olaiya, D. Petyt, T. Reis, T. Schuh, C.H. Shepherd-Themistocleous, I.R. Tomalin, T. Williams

Imperial College, London, United Kingdom

R. Bainbridge, P. Bloch, S. Bonomally, J. Borg, S. Breeze, O. Buchmuller, V. Cepaitis, G.S. Chahal⁸⁵, D. Colling, P. Dauncey, G. Davies, M. Della Negra, S. Fayer, G. Fedi, G. Hall, M.H. Hassanshahi, G. Iles, J. Langford, L. Lyons, A.-M. Magnan, S. Malik, A. Martelli, D.G. Monk, J. Nash⁸⁶, M. Pesaresi, D.M. Raymond, A. Richards, A. Rose, E. Scott, C. Seez, A. Shtipliyski, A. Tapper, K. Uchida, T. Virdee²⁰, M. Vojinovic, N. Wardle, S.N. Webb, D. Winterbottom, A.G. Zecchinelli

Brunel University, Uxbridge, United Kingdom

K. Coldham, J.E. Cole, A. Khan, P. Kyberd, I.D. Reid, L. Teodorescu, S. Zahid

Baylor University, Waco, USA

S. Abdullin, A. Brinkerhoff, B. Caraway, J. Dittmann, K. Hatakeyama, A.R. Kanuganti, B. McMaster, N. Pastika, M. Saunders, S. Sawant, C. Sutantawibul, J. Wilson

Catholic University of America, Washington, DC, USA

R. Bartek, A. Dominguez, R. Uniyal, A.M. Vargas Hernandez

The University of Alabama, Tuscaloosa, USA

A. Buccilli, S.I. Cooper, D. Di Croce, S.V. Gleyzer, C. Henderson, C.U. Perez, P. Rumerio⁸⁷, C. West

Boston University, Boston, USA

A. Akpınar, A. Albert, D. Arcaro, C. Cosby, Z. Demiragli, E. Fontanesi, D. Gastler, J. Rohlf, K. Salyer, D. Sperka, D. Spitzbart, I. Suarez, A. Tsatsos, S. Yuan, D. Zou

Brown University, Providence, USA

G. Benelli, B. Burkle, X. Coubez²¹, D. Cutts, M. Hadley, U. Heintz, J.M. Hogan⁸⁸, G. Landsberg, K.T. Lau, M. Lukasik, J. Luo, M. Narain, S. Sagir⁸⁹, E. Usai, W.Y. Wong, X. Yan, D. Yu, W. Zhang

University of California, Davis, Davis, USA

J. Bonilla, C. Brainerd, R. Breedon, M. Calderon De La Barca Sanchez, M. Chertok, J. Conway, P.T. Cox, R. Erbacher, G. Haza, F. Jensen, O. Kukral, R. Lander, M. Mulhearn, D. Pellett, B. Regnery, D. Taylor, Y. Yao, F. Zhang

University of California, Los Angeles, USA

M. Bachtis, R. Cousins, A. Datta, D. Hamilton, J. Hauser, M. Ignatenko, M.A. Iqbal, T. Lam, W.A. Nash, S. Regnard, D. Saltzberg, B. Stone, V. Valuev

University of California, Riverside, Riverside, USA

K. Burt, Y. Chen, R. Clare, J.W. Gary, M. Gordon, G. Hanson, G. Karapostoli, O.R. Long, N. Manganeli, M. Olmedo Negrete, W. Si, S. Wimpenny, Y. Zhang

University of California, San Diego, La Jolla, USA

J.G. Branson, P. Chang, S. Cittolin, S. Cooperstein, N. Deelen, D. Diaz, J. Duarte, R. Gerosa, L. Giannini, D. Gilbert, J. Guiang, R. Kansal, V. Krutelyov, R. Lee, J. Letts, M. Masciovecchio, S. May, M. Pieri, B.V. Sathia Narayanan, V. Sharma, M. Tadel, A. Vartak, F. Würthwein, Y. Xiang, A. Yagil

University of California, Santa Barbara - Department of Physics, Santa Barbara, USA

N. Amin, C. Campagnari, M. Citron, A. Dorsett, V. Dutta, J. Incandela, M. Kilpatrick, J. Kim, B. Marsh, H. Mei, M. Oshiro, M. Quinnan, J. Richman, U. Sarica, J. Sheplock, D. Stuart, S. Wang

California Institute of Technology, Pasadena, USA

A. Bornheim, O. Cerri, I. Dutta, J.M. Lawhorn, N. Lu, J. Mao, H.B. Newman, J. Ngadiuba, T.Q. Nguyen, M. Spiropulu, J.R. Vlimant, C. Wang, S. Xie, Z. Zhang, R.Y. Zhu

Carnegie Mellon University, Pittsburgh, USA

J. Alison, S. An, M.B. Andrews, P. Bryant, T. Ferguson, A. Harilal, C. Liu, T. Mudholkar, M. Paulini, A. Sanchez

University of Colorado Boulder, Boulder, USA

J.P. Cumalat, W.T. Ford, A. Hassani, E. MacDonald, R. Patel, A. Perloff, C. Savard, K. Stenson, K.A. Ulmer, S.R. Wagner

Cornell University, Ithaca, USA

J. Alexander, S. Bright-thonney, Y. Cheng, D.J. Cranshaw, S. Hogan, J. Monroy, J.R. Patterson, D. Quach, J. Reichert, M. Reid, A. Ryd, W. Sun, J. Thom, P. Wittich, R. Zou

Fermi National Accelerator Laboratory, Batavia, USA

M. Albrow, M. Alyari, G. Apollinari, A. Apresyan, A. Apyan, S. Banerjee, L.A.T. Bauerdick, D. Berry, J. Berryhill, P.C. Bhat, K. Burkett, J.N. Butler, A. Canepa, G.B. Cerati, H.W.K. Cheung, F. Chlebana, M. Cremonesi, K.F. Di Petrillo, V.D. Elvira, Y. Feng, J. Freeman, Z. Gecse, L. Gray, D. Green, S. Grünendahl, O. Gutsche, R.M. Harris, R. Heller, T.C. Herwig, J. Hirschauer, B. Jayatilaka, S. Jindariani, M. Johnson, U. Joshi, T. Klijnsma, B. Klima, K.H.M. Kwok, S. Lammel, D. Lincoln, R. Lipton, T. Liu, C. Madrid, K. Maeshima, C. Mantilla, D. Mason, P. McBride, P. Merkel, S. Mrenna, S. Nahn, V. O'Dell, V. Papadimitriou, K. Pedro, C. Pena⁵⁷, O. Prokofyev, F. Ravera, A. Reinsvold Hall, L. Ristori, B. Schneider, E. Sexton-Kennedy, N. Smith, A. Soha, W.J. Spalding, L. Spiegel, S. Stoynev, J. Strait, L. Taylor, S. Tkaczyk, N.V. Tran, L. Uplegger, E.W. Vaandering, H.A. Weber

University of Florida, Gainesville, USA

D. Acosta, P. Avery, D. Bourilkov, L. Cadamuro, V. Cherepanov, F. Errico, R.D. Field, D. Guerrero, B.M. Joshi, M. Kim, E. Koenig, J. Konigsberg, A. Korytov, K.H. Lo, K. Matchev, N. Menendez, G. Mitselmakher, A. Muthirakalayil Madhu, N. Rawal, D. Rosenzweig, S. Rosenzweig, K. Shi, J. Sturdy, J. Wang, E. Yigitbasi, X. Zuo

Florida State University, Tallahassee, USA

T. Adams, A. Askew, R. Habibullah, V. Hagopian, K.F. Johnson, R. Khurana, T. Kolberg, G. Martinez, H. Prosper, C. Schiber, O. Viazlo, R. Yohay, J. Zhang

Florida Institute of Technology, Melbourne, USA

M.M. Baarmand, S. Butalla, T. Elkafrawy¹⁶, M. Hohlmann, R. Kumar Verma, D. Noonan, M. Rahmani, F. Yumiceva

University of Illinois at Chicago (UIC), Chicago, USA

M.R. Adams, H. Becerril Gonzalez, R. Cavanaugh, X. Chen, S. Dittmer, O. Evdokimov, C.E. Gerber, D.A. Hangal, D.J. Hofman, A.H. Merrit, C. Mills, G. Oh, T. Roy, S. Rudrabhatla, M.B. Tonjes, N. Varelas, J. Viinikainen, X. Wang, Z. Wu, Z. Ye

The University of Iowa, Iowa City, USA

M. Alhusseini, K. Dilsiz⁹⁰, R.P. Gandrajula, O.K. Köseyan, J.-P. Merlo, A. Mestvirishvili⁹¹, J. Nachtman, H. Ogul⁹², Y. Onel, A. Penzo, C. Snyder, E. Tiras⁹³

Johns Hopkins University, Baltimore, USA

O. Amram, B. Blumenfeld, L. Corcodilos, J. Davis, M. Eminizer, A.V. Gritsan, S. Kyriacou, P. Maksimovic, J. Roskes, M. Swartz, T.Á. Vámi

The University of Kansas, Lawrence, USA

A. Abreu, J. Anguiano, C. Baldenegro Barrera, P. Baringer, A. Bean, A. Bylinkin, Z. Flowers, T. Isidori, S. Khalil, J. King, G. Krintiras, A. Kropivnitskaya, M. Lazarovits, C. Lindsey, J. Marquez, N. Minafra, M. Murray, M. Nickel, C. Rogan, C. Royon, R. Salvatico, S. Sanders, E. Schmitz, C. Smith, J.D. Tapia Takaki, Q. Wang, Z. Warner, J. Williams, G. Wilson

Kansas State University, Manhattan, USA

S. Duric, A. Ivanov, K. Kaadze, D. Kim, Y. Maravin, T. Mitchell, A. Modak, K. Nam

Lawrence Livermore National Laboratory, Livermore, USA

F. Rebassoo, D. Wright

University of Maryland, College Park, USA

E. Adams, A. Baden, O. Baron, A. Belloni, S.C. Eno, N.J. Hadley, S. Jabeen, R.G. Kellogg, T. Koeth, A.C. Mignerey, S. Nabili, M. Seidel, A. Skuja, L. Wang, K. Wong

Massachusetts Institute of Technology, Cambridge, USA

D. Abercrombie, G. Andreassi, R. Bi, S. Brandt, W. Busza, I.A. Cali, Y. Chen, M. D'Alfonso, J. Eysermans, C. Freer, G. Gomez Ceballos, M. Goncharov, P. Harris, M. Hu, M. Klute, D. Kovalskyi, J. Krupa, Y.-J. Lee, B. Maier, C. Mironov, C. Paus, D. Rankin, C. Roland, G. Roland, Z. Shi, G.S.F. Stephans, K. Tatar, J. Wang, Z. Wang, B. Wyslouch

University of Minnesota, Minneapolis, USA

R.M. Chatterjee, A. Evans, P. Hansen, J. Hiltbrand, Sh. Jain, M. Krohn, Y. Kubota, J. Mans, M. Revering, R. Rusack, R. Saradhy, N. Schroeder, N. Strobbe, M.A. Wadud

University of Nebraska-Lincoln, Lincoln, USA

K. Bloom, M. Bryson, S. Chauhan, D.R. Claes, C. Fangmeier, L. Finco, F. Golf, C. Joo, I. Kravchenko, M. Musich, I. Reed, J.E. Siado, G.R. Snow[†], W. Tabb, F. Yan

State University of New York at Buffalo, Buffalo, USA

G. Agarwal, H. Bandyopadhyay, L. Hay, I. Iashvili, A. Kharchilava, C. McLean, D. Nguyen, J. Pekkanen, S. Rappoccio, A. Williams

Northeastern University, Boston, USA

G. Alverson, E. Barberis, Y. Haddad, A. Hortiangtham, J. Li, G. Madigan, B. Marzocchi, D.M. Morse, V. Nguyen, T. Orimoto, A. Parker, L. Skinnari, A. Tishelman-Charny, T. Wamorkar, B. Wang, A. Wisecarver, D. Wood

Northwestern University, Evanston, USA

S. Bhattacharya, J. Bueghly, Z. Chen, A. Gilbert, T. Gunter, K.A. Hahn, Y. Liu, N. Odell, M.H. Schmitt, M. Velasco

University of Notre Dame, Notre Dame, USA

R. Band, R. Bucci, A. Das, N. Dev, R. Goldouzian, M. Hildreth, K. Hurtado Anampa, C. Jessop, K. Lannon, J. Lawrence, N. Loukas, D. Lutton, N. Marinelli, I. Mcalister, T. McCauley, F. Meng, K. Mohrman, Y. Musienko⁵⁰, R. Ruchti, P. Siddireddy, A. Townsend, M. Wayne, A. Wightman, M. Wolf, M. Zarucki, L. Zygala

The Ohio State University, Columbus, USA

B. Bylsma, B. Cardwell, L.S. Durkin, B. Francis, C. Hill, M. Nunez Ornelas, K. Wei, B.L. Winer, B.R. Yates

Princeton University, Princeton, USA

F.M. Addesa, B. Bonham, P. Das, G. Dezoort, P. Elmer, A. Frankenthal, B. Greenberg,

N. Haubrich, S. Higginbotham, A. Kalogeropoulos, G. Kopp, S. Kwan, D. Lange, M.T. Lucchini, D. Marlow, K. Mei, I. Ojalvo, J. Olsen, C. Palmer, D. Stickland, C. Tully

University of Puerto Rico, Mayaguez, USA

S. Malik, S. Norberg

Purdue University, West Lafayette, USA

A.S. Bakshi, V.E. Barnes, R. Chawla, S. Das, L. Gutay, M. Jones, A.W. Jung, S. Karmarkar, M. Liu, G. Negro, N. Neumeister, G. Paspalaki, C.C. Peng, S. Piperov, A. Purohit, J.F. Schulte, M. Stojanovic¹⁷, J. Thieman, F. Wang, R. Xiao, W. Xie

Purdue University Northwest, Hammond, USA

J. Dolen, N. Parashar

Rice University, Houston, USA

A. Baty, M. Decaro, S. Dildick, K.M. Ecklund, S. Freed, P. Gardner, F.J.M. Geurts, A. Kumar, W. Li, B.P. Padley, R. Redjimi, W. Shi, A.G. Stahl Leitton, S. Yang, L. Zhang, Y. Zhang

University of Rochester, Rochester, USA

A. Bodek, P. de Barbaro, R. Demina, J.L. Dulemba, C. Fallon, T. Ferbel, M. Galanti, A. Garcia-Bellido, O. Hindrichs, A. Khukhunaishvili, E. Ranken, R. Taus

Rutgers, The State University of New Jersey, Piscataway, USA

B. Chiarito, J.P. Chou, A. Gandrakota, Y. Gershtein, E. Halkiadakis, A. Hart, M. Heindl, O. Karacheban²⁴, I. Laflotte, A. Lath, R. Montalvo, K. Nash, M. Osherson, S. Salur, S. Schnetzer, S. Somalwar, R. Stone, S.A. Thayil, S. Thomas, H. Wang

University of Tennessee, Knoxville, USA

H. Acharya, A.G. Delannoy, S. Spanier

Texas A&M University, College Station, USA

O. Bouhali⁹⁴, M. Dalchenko, A. Delgado, R. Eusebi, J. Gilmore, T. Huang, T. Kamon⁹⁵, H. Kim, S. Luo, S. Malhotra, R. Mueller, D. Overton, D. Rathjens, A. Safonov

Texas Tech University, Lubbock, USA

N. Akchurin, J. Damgov, V. Hegde, S. Kunori, K. Lamichhane, S.W. Lee, T. Mengke, S. Muthumuni, T. Peltola, I. Volobouev, Z. Wang, A. Whitbeck

Vanderbilt University, Nashville, USA

E. Appelt, S. Greene, A. Gurrola, W. Johns, A. Melo, H. Ni, K. Padeken, F. Romeo, P. Sheldon, S. Tuo, J. Velkovska

University of Virginia, Charlottesville, USA

M.W. Arenton, B. Cox, G. Cummings, J. Hakala, R. Hirosky, M. Joyce, A. Ledovskoy, A. Li, C. Neu, B. Tannenwald, S. White, E. Wolfe

Wayne State University, Detroit, USA

N. Poudyal

University of Wisconsin - Madison, Madison, WI, USA

K. Black, T. Bose, J. Buchanan, C. Caillol, S. Dasu, I. De Bruyn, P. Everaerts, F. Fienga, C. Galloni, H. He, M. Herndon, A. Hervé, U. Hussain, A. Lanaro, A. Loeliger, R. Loveless, J. Madhusudanan Sreekala, A. Mallampalli, A. Mohammadi, D. Pinna, A. Savin, V. Shang, V. Sharma, W.H. Smith, D. Teague, S. Trembath-reichert, W. Vetens

†: Deceased

- 1: Also at TU Wien, Wien, Austria
- 2: Also at Institute of Basic and Applied Sciences, Faculty of Engineering, Arab Academy for Science, Technology and Maritime Transport, Alexandria, Egypt, Alexandria, Egypt
- 3: Also at Université Libre de Bruxelles, Bruxelles, Belgium
- 4: Also at Universidade Estadual de Campinas, Campinas, Brazil
- 5: Also at Federal University of Rio Grande do Sul, Porto Alegre, Brazil
- 6: Also at University of Chinese Academy of Sciences, Beijing, China
- 7: Also at Department of Physics, Tsinghua University, Beijing, China, Beijing, China
- 8: Also at UFMS, Nova Andradina, Brazil
- 9: Also at Nanjing Normal University Department of Physics, Nanjing, China
- 10: Now at The University of Iowa, Iowa City, USA
- 11: Also at Institute for Theoretical and Experimental Physics named by A.I. Alikhanov of NRC 'Kurchatov Institute', Moscow, Russia
- 12: Also at Joint Institute for Nuclear Research, Dubna, Russia
- 13: Also at Helwan University, Cairo, Egypt
- 14: Now at Zewail City of Science and Technology, Zewail, Egypt
- 15: Also at British University in Egypt, Cairo, Egypt
- 16: Now at Ain Shams University, Cairo, Egypt
- 17: Also at Purdue University, West Lafayette, USA
- 18: Also at Université de Haute Alsace, Mulhouse, France
- 19: Also at Erzincan Binali Yildirim University, Erzincan, Turkey
- 20: Also at CERN, European Organization for Nuclear Research, Geneva, Switzerland
- 21: Also at RWTH Aachen University, III. Physikalisches Institut A, Aachen, Germany
- 22: Also at University of Hamburg, Hamburg, Germany
- 23: Also at Department of Physics, Isfahan University of Technology, Isfahan, Iran, Isfahan, Iran
- 24: Also at Brandenburg University of Technology, Cottbus, Germany
- 25: Also at Skobeltsyn Institute of Nuclear Physics, Lomonosov Moscow State University, Moscow, Russia
- 26: Also at Physics Department, Faculty of Science, Assiut University, Assiut, Egypt
- 27: Also at Karoly Robert Campus, MATE Institute of Technology, Gyongyos, Hungary
- 28: Also at Institute of Physics, University of Debrecen, Debrecen, Hungary, Debrecen, Hungary
- 29: Also at Institute of Nuclear Research ATOMKI, Debrecen, Hungary
- 30: Also at MTA-ELTE Lendület CMS Particle and Nuclear Physics Group, Eötvös Loránd University, Budapest, Hungary, Budapest, Hungary
- 31: Also at Wigner Research Centre for Physics, Budapest, Hungary
- 32: Also at IIT Bhubaneswar, Bhubaneswar, India, Bhubaneswar, India
- 33: Also at Institute of Physics, Bhubaneswar, India
- 34: Also at G.H.G. Khalsa College, Punjab, India
- 35: Also at Shoolini University, Solan, India
- 36: Also at University of Hyderabad, Hyderabad, India
- 37: Also at University of Visva-Bharati, Santiniketan, India
- 38: Also at Indian Institute of Technology (IIT), Mumbai, India
- 39: Also at Deutsches Elektronen-Synchrotron, Hamburg, Germany
- 40: Also at Sharif University of Technology, Tehran, Iran
- 41: Also at Department of Physics, University of Science and Technology of Mazandaran, Behshahr, Iran

-
- 42: Now at INFN Sezione di Bari ^a, Università di Bari ^b, Politecnico di Bari ^c, Bari, Italy
- 43: Also at Italian National Agency for New Technologies, Energy and Sustainable Economic Development, Bologna, Italy
- 44: Also at Centro Siciliano di Fisica Nucleare e di Struttura Della Materia, Catania, Italy
- 45: Also at Università di Napoli 'Federico II', NAPOLI, Italy
- 46: Also at Consiglio Nazionale delle Ricerche - Istituto Officina dei Materiali, PERUGIA, Italy
- 47: Also at Riga Technical University, Riga, Latvia, Riga, Latvia
- 48: Also at Consejo Nacional de Ciencia y Tecnología, Mexico City, Mexico
- 49: Also at IRFU, CEA, Université Paris-Saclay, Gif-sur-Yvette, France
- 50: Also at Institute for Nuclear Research, Moscow, Russia
- 51: Now at National Research Nuclear University 'Moscow Engineering Physics Institute' (MEPhI), Moscow, Russia
- 52: Also at Institute of Nuclear Physics of the Uzbekistan Academy of Sciences, Tashkent, Uzbekistan
- 53: Also at St. Petersburg State Polytechnical University, St. Petersburg, Russia
- 54: Also at University of Florida, Gainesville, USA
- 55: Also at Imperial College, London, United Kingdom
- 56: Also at Moscow Institute of Physics and Technology, Moscow, Russia, Moscow, Russia
- 57: Also at California Institute of Technology, Pasadena, USA
- 58: Also at Budker Institute of Nuclear Physics, Novosibirsk, Russia
- 59: Also at Faculty of Physics, University of Belgrade, Belgrade, Serbia
- 60: Also at Trincomalee Campus, Eastern University, Sri Lanka, Nilaveli, Sri Lanka
- 61: Also at INFN Sezione di Pavia ^a, Università di Pavia ^b, Pavia, Italy, Pavia, Italy
- 62: Also at National and Kapodistrian University of Athens, Athens, Greece
- 63: Also at Ecole Polytechnique Fédérale Lausanne, Lausanne, Switzerland
- 64: Also at Universität Zürich, Zurich, Switzerland
- 65: Also at Stefan Meyer Institute for Subatomic Physics, Vienna, Austria, Vienna, Austria
- 66: Also at Laboratoire d'Annecy-le-Vieux de Physique des Particules, IN2P3-CNRS, Annecy-le-Vieux, France
- 67: Also at Şırnak University, Sirnak, Turkey
- 68: Also at Near East University, Research Center of Experimental Health Science, Nicosia, Turkey
- 69: Also at Konya Technical University, Konya, Turkey
- 70: Also at Istanbul University - Cerrahpasa, Faculty of Engineering, Istanbul, Turkey
- 71: Also at Piri Reis University, Istanbul, Turkey
- 72: Also at Adiyaman University, Adiyaman, Turkey
- 73: Also at Ozyegin University, Istanbul, Turkey
- 74: Also at Izmir Institute of Technology, Izmir, Turkey
- 75: Also at Necmettin Erbakan University, Konya, Turkey
- 76: Also at Bozok Universititesi Rektörlüğü, Yozgat, Turkey, Yozgat, Turkey
- 77: Also at Marmara University, Istanbul, Turkey
- 78: Also at Milli Savunma University, Istanbul, Turkey
- 79: Also at Kafkas University, Kars, Turkey
- 80: Also at Istanbul Bilgi University, Istanbul, Turkey
- 81: Also at Hacettepe University, Ankara, Turkey
- 82: Also at Rutherford Appleton Laboratory, Didcot, United Kingdom
- 83: Also at Vrije Universiteit Brussel, Brussel, Belgium
- 84: Also at School of Physics and Astronomy, University of Southampton, Southampton, United Kingdom

- 85: Also at IPPP Durham University, Durham, United Kingdom
- 86: Also at Monash University, Faculty of Science, Clayton, Australia
- 87: Also at Università di Torino, TORINO, Italy
- 88: Also at Bethel University, St. Paul, Minneapolis, USA, St. Paul, USA
- 89: Also at Karamanoğlu Mehmetbey University, Karaman, Turkey
- 90: Also at Bingol University, Bingol, Turkey
- 91: Also at Georgian Technical University, Tbilisi, Georgia
- 92: Also at Sinop University, Sinop, Turkey
- 93: Also at Erciyes University, KAYSERI, Turkey
- 94: Also at Texas A&M University at Qatar, Doha, Qatar
- 95: Also at Kyungpook National University, Daegu, Korea, Daegu, Korea